



**HAL**  
open science

## On the heterogeneous impacts of the COVID-19 lockdown on US unemployment

Malak Kandoussi, François Langot

► **To cite this version:**

Malak Kandoussi, François Langot. On the heterogeneous impacts of the COVID-19 lockdown on US unemployment. 2021. hal-03107369

**HAL Id: hal-03107369**

**<https://hal.science/hal-03107369v1>**

Preprint submitted on 12 Jan 2021

**HAL** is a multi-disciplinary open access archive for the deposit and dissemination of scientific research documents, whether they are published or not. The documents may come from teaching and research institutions in France or abroad, or from public or private research centers.

L'archive ouverte pluridisciplinaire **HAL**, est destinée au dépôt et à la diffusion de documents scientifiques de niveau recherche, publiés ou non, émanant des établissements d'enseignement et de recherche français ou étrangers, des laboratoires publics ou privés.

# On the heterogeneous impacts of the COVID-19 lockdown on US unemployment

Malak Kandoussi\*

EPEE, Université Paris-Saclay, University of Evry

François Langot†

Le Mans University (Gains-TEPP & IRA), IUF, PSE, IZA

January 2021

## Abstract

We develop a matching model that predicts the impact of the COVID-19 lockdown on US unemployment, while accounting for the contrasted impacts across various job types. The model is calibrated on the subprime experience and is then used to identify the job-specific lockdown shocks, using observed worker flows by diploma. The model persistence — which is significantly larger than in the Diamond–Mortensen–Pissarides model — is dampened by CARES act that facilitates the use of temporary separations. Counterfactual experiments show that time-varying risk, hiring cost externalities, and wage rigidity are needed to account for these crises.

**Keywords:** COVID-19, unemployment, search and matching, worker heterogeneity

**JEL Classifications:** E24, E32, J64

---

\*Corresponding author: [malak.kandoussi@univ-evry.fr](mailto:malak.kandoussi@univ-evry.fr). Université Paris-Saclay, Université d'Evry, EPEE, 91025, Evry-Courcouronnes, France.

†F. Langot acknowledges financial support from the *Institut Universitaire de France*, from the *PANORisk* grant, and from the EUR grant ANR-17-EURE-0001.

# 1 Introduction

The COVID-19 crisis has led to severe lockdown measures, on account of heightened health and sanitation concerns. These sanitation measures have generated unprecedented

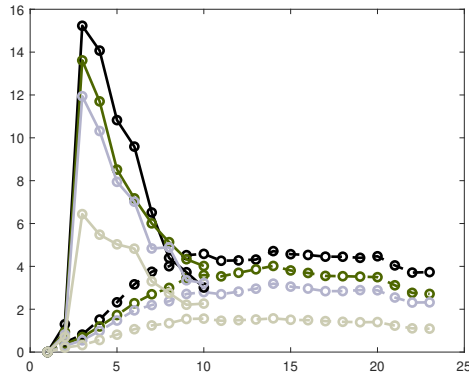


Figure 1: **Rises in monthly unemployment rates by diploma after a crisis.** Increases in percentage points relative to the pre-crisis levels. Black: Less than High School diploma. Khaki: High School diploma. Gray: College degree. Camel: Bachelor and more degree. Lines: COVID-19 crisis. Dotted lines: Subprime crisis.

increase in US unemployment. Moreover, these measures did not affect all workers in the same way, and so they have generated an unequal rise in unemployment risk (see Figure 1). Perhaps more so than in previous crises, this COVID-19 crisis, on account of both its

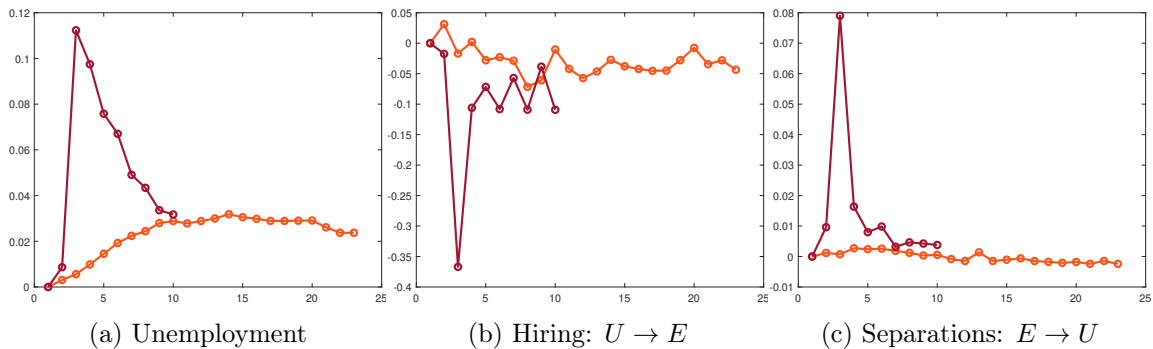


Figure 2: **Dynamics of monthly workers flows and stock after a crisis.** Red: COVID-19 crisis. Orange: Subprime crisis. Increases in percentage points relative to the pre-crisis levels.

brutality and magnitude (see Figure 2), challenges the Diamond–Mortensen–Pissarides (DMP) model, the framework typically used to analyze unemployment dynamics.<sup>1</sup> Moreover, the two last crises have induced very different changes in workers’ flows (see Figure

<sup>1</sup>Our work thus pursues those of Nicolas Petrosky and Zhang (2020), Hall (2017) and Hall and Kudlyak (2020), which shows how the DMP model can explain previous crises.

2) which makes it harder to identify a parsimonious model able to explain this particular succession of crises.

In the current study, we develop a model that reproduces the impact of the lockdown on heterogeneous workers in the United States. We propose an original extension of the DMP model, which introduces *(H1)* worker heterogeneity, *(H2)* time-varying microeconomic risks over the business cycle, *(H3)* congestion externalities in the hiring costs, and *(H4)* real-wage rigidity. This model is calibrated to reproduce the impact of the 2008 sub-prime crisis on unemployment and workers' flows. Using this calibrated model, we reveal the COVID-19 shocks, specific to each type of activity, that allow it to fit the monthly labor market data since March 2020. The constraints on market exchanges induced by the lockdown are modeled as reductions in Total Factor Productivity (TFP), while the measures facilitating temporary layoffs induced by the Coronavirus Aid, Relief, and Economic Security (CARES) act are modeled as temporary reductions in unit costs of hiring. Taking advantage from our structural approach, we estimate the true lockdown induced constraints for different jobs, as well as the effectiveness of the CARES act to damp the impact of this recession on unemployment risk of different workers.

The main challenge consists in extending the DMP model such that it explains large crises. Doing so is challenging for this textbook model, for the following four reasons. First, unemployment rate more than doubled within one month of the COVID-19 crisis, and this underscores the very large elasticity of unemployment in relation to the business cycle. Second, in the past, in the wake of crisis, unemployment rate has never experienced a rapid decline, and this suggests that matching externalities are not sufficient to explain unemployment persistence.<sup>2</sup> Third, the increase in unemployment risk during the crisis depends highly on the worker type (i.e., heterogeneity matters).<sup>3,4</sup> Fourth, the distribution of job productivity for each job varies during the business cycle, with heterogeneity

---

<sup>2</sup>Hall and Kudlyak (2020) show that, during periods of recovery over the past 70 years, we can see a 0.5-percentage-point reduction in unemployment per year, which suggests that the current crisis would be resolved within 15 years.

<sup>3</sup>Robin (2011) and Lise and Robin (2017) show that heterogeneity matters in accounting for aggregate labor dynamics. See also Ferraro (2018) & (2000) and Adjemian et al. (2019).

<sup>4</sup>Empirical investigations of Adams-Prassl et al. (2020) show that, for some occupations, workers' ability to undertake a large percentage of their tasks from home (i.e., "telework") is limited; this is especially true for low-income professions. Using the European Union labor force survey, Fana et al. (2020) show that most of the negative effects of the lockdown measures are concentrated on less-skilled workers. Indeed, the sectors forcefully closed by decree of their decomposition are characterized by low wages and high separation rates. These findings suggest that worker heterogeneity matters in the evaluation of the lockdown impacts on unemployment.

increasing during times of recession.<sup>5</sup>

To explain the impact of various crises on the US unemployment, an extended version of the DMP model that included assumptions  $(H1)$ - $(H4)$  is developed for an economy where workers have heterogeneous educational attainments.<sup>6</sup> We start by showing that our model can reproduce the impact of the 2008 subprime crisis. Although this crisis is not similar with the COVID-19 ones, having a model that reproduces the observed asymmetric adjustments of the US labor market (i.e., rapid increase and slow recovery), and the unemployment risk inequalities (i.e., the least educated are strongly impacted), is essential to forecast the impact of the current crisis. Using this calibrated model, we identify the size of the shocks needed to reproduce the COVID-19 crisis. We show that the “direct” impact of the lockdown measures significantly differs across education levels: in April 2020, workers without a high school diploma suffered from an almost 28% drop in their TFP, while those holding a bachelor degree or more saw their TFP decreases by only 3%. The negative impact of the lockdown on worker TFP thus lies between these two extreme cases for the two other worker types (i.e., -23% and -18% for those with a high school diploma and college diploma, respectively ). When the lockdown ended in May, productivity levels returned to their precrisis levels. We also show that the CARES act raises unemployment by facilitating separations: the inducement of temporary layoffs allowed by CARES act explains 32% of total separations from March to November. However, the CARES act significantly reduces the average duration of unemployment (from more than 3 weeks in April to 1 week in June), which was one of its priority objectives. Finally, we show that for workers with less than a high school diploma, wage losses amount to 12% three months after the first shock; these losses attenuate as the postcrisis time horizon increases (i.e., even 24 months after the crisis, it remains at 4%), while for those with at least a bachelor degree, the losses amount to 6%. Given that precrisis labor income inequalities were already high, it therefore appears that this COVID-19 crisis will only exacerbate them, even if the effect measured here were only transitory.

We show that all extensions of the DMP model are crucial in explaining US labor market

---

<sup>5</sup>This fact has been underscored by Bloom (2009).

<sup>6</sup>Heterogeneity in educational attainment is fixed over time so as it is consistent with a model that lacks mobility among submarkets. This distinguishes our modeling strategy from that of Gregory et al. (2020), who define three worker groups on the basis of their “performance” with respect to labor market transitions. Heterogeneity by education level seems to be well suited to predicting workers’ type-specific effects of the lockdown measures, and their heterogeneous effects (see Adams-Prassl et al. (2020) or Fana et al. (2020)).

fluctuations. First, worker heterogeneity matters, because only a small fraction of the population can be highly sensitive to the business cycle and, despite its small mass, it generates large unemployment rates in times of recessions through larger separations. Second, time-varying microeconomic risk *à la* Bloom et al. (2018) (countercyclical risk) helps the model generate persistent separations after the lockdown, as seen in US worker flow data.<sup>7</sup> Third, our counterfactual simulations show that the speed of convergence of the DMP model is too fast compared to what it is actually observed; this leads to large underestimations of the impact of recessions: the introduction of congestion externality *à la* Hall and Kudlyak (2020) are thus crucial. Finally, as wage rigidities keep wages close to their precrisis levels, firms continue to dismiss workers, even after the lockdown. As a corollary, the COVID-19 shocks “estimated” by each restricted model (i.e., our model, where one of these channels is shut off) are significantly different from those deduced from our benchmark model, where a larger persistence in these forcing variables allows us to compensate for the lack of propagation mechanisms in these restricted models.

There is already a significant literature studying the impact of the COVID-19 crisis on the US labor market. Numerous empirical studies, including Gallant et al. (2020), Barrero et al. (2020), Bartik et al. (2020) among others, attest the unprecedented amplitude of the drop in hirings and the increase in separations, both leading to the spike in US unemployment. Other works based on structural approaches improve our understanding of the propagation mechanisms of this crisis, such as Gregory et al. (2020), Hall and Kudlyak (2020) or Bernstein et al. (2020).<sup>8</sup> Our paper complements these previous studies by determining the most parsimonious structural model making it possible to quantitatively account for the impact of the COVID-19 crisis on the US labor market, in terms of its amplitude, its persistence and the resulting inequalities.

The remainder of this paper is organized as follows. Section 2 presents the model, and Section 3 discusses calibration and model-fits regarding the 2008 subprime crisis data. Section 4.1 presents projections for the impact of COVID-19 on the US labor market; at the end of this section, we discuss alternative scenarios for the lockdown that would be longer but less stricter. Finally, Section 5 concludes.

---

<sup>7</sup>See Baker et al. (2020) for an analysis of changes in uncertainty since the start of the COVID-19 crisis. Den Haan et al. (2020) show that time-varying risk improves the ability of the DMP model to explain US unemployment dynamics.

<sup>8</sup>Let us notice that Kapicka and Rupert (2020) and Birinci et al. (2020) integrate DMP type models into epidemiological models in order to better analyze the interplay between public health policies and economic efficiency. This very interesting normative approach is left beyond the scope of the present paper.

## 2 Model

We aim to analyze the effect of aggregated and disaggregated shocks within a Search and Matching model, using a general equilibrium approach.<sup>9</sup>

On the labor market, we add two important externalities with respect to the canonical DMP model—both of which aim to account for the greatest difficulties in times of crisis—to derive sound workforce information. First, it is assumed that units' recruitment costs will increase when unemployment diverges from its long-term value, and this introduces a congestion externality on hirings. Second, the dispersion of idiosyncratic productivities is assumed to be greater when unemployment diverges from its long-term value, which makes microeconomic uncertainty countercyclical. The labor markets are segmented, with each skill achieving only one task for producing one specific good. The workers are heterogeneous with respect to their educational attainment  $s$ . The share of each skill (educational attainment) within the mass of workers is  $\omega_s$ .

On the financial market, we assume that only a mass  $1 - \varphi$  of the population have access to financial markets. Hence, the financial needs of companies wishing to reopen after activity cessations are supplied by savers.

On the goods market, the household's choice of her consumption basket generate interactions among different labor markets, and this makes it possible to determine the relative prices of goods in each period.

### 2.1 Consumers

The labor market for each skill  $s \in \overline{\mathcal{S}}$  is segmented, and we assume that each skill  $s$  can produce only one type of product  $j$ . Hence, there is a perfect correspondence between  $s$  and  $j$ . The preferences are defined over a set of goods  $j \in \mathcal{J}_t \Leftrightarrow s \in \mathcal{S}_t$ . When all markets are open,  $\mathcal{S}_t$  is  $s = 1, \dots, S$ , where  $S$  is the maximal number of varieties bounded by the number of skills  $S$ . Otherwise,  $\dim(\mathcal{S}_t) < S$  with a cardinal denoted  $S_{n,t} < S$ .

---

<sup>9</sup>We make abusive use of the term "shock" because we will perform deterministic simulations of unanticipated sequences of exogenous variables.

### 2.1.1 Financially unconstrained agents: the capitalist

The capitalists aim to maximize the sum of their discounted utility, which is given by

$$\sum_{t=0}^{\infty} \beta_t^t \left( \frac{(C_t^K)^{1-\nu}}{1-\nu} + A_b B_t \right) \quad \text{with } C_t^K = S_{n,t}^{\frac{1}{1-\sigma}} \left( \sum_{s \in \mathcal{S}_t} (C_{s,t}^K)^{\frac{\sigma-1}{\sigma}} \right)^{\frac{\sigma}{\sigma-1}},$$

where  $C_t^K$  denotes the basket of consumption goods and  $B_t$  the composite storable goods that provide utility. The consumer price index (CPI) is defined by  $p_t = \left( \frac{1}{S_{n,t}} \sum_{s \in \mathcal{S}_t} p_{s,t}^{1-\sigma} \right)^{\frac{1}{1-\sigma}}$  and is normalized to unity ( $p_t = 1, \forall t$ ). Storable goods accumulate as follows:

$$B_{t+1} = (1-\delta)B_t + S_{n,t}^{\frac{1}{1-\sigma}} \left( \sum_{s \in \mathcal{S}_t} (I_{s,t}^K)^{\frac{\sigma-1}{\sigma}} \right)^{\frac{\sigma}{\sigma-1}} - \frac{\varphi}{1-\varphi} \sum_{s \notin \mathcal{S}_t} \omega_s \psi_s \kappa_{s,t} V_{s,t},$$

where we assume that a capitalist finances the firm's reopening costs (i.e., the last term of the last equation). Because markets  $s \notin \mathcal{S}_t$  are not open at this period  $t$ , the unit cost of each transaction between the capitalist and a reopening firm is  $\psi_s$ . The budgetary constraint of this representative agent is

$$\begin{aligned} C_t^K + I_t^K &= \frac{\varphi}{1-\varphi} \left( \sum_{s \in \mathcal{S}_t} \omega_s D_{s,t} - \sum_{s \notin \mathcal{S}_t} \omega_s \psi_s \kappa_{s,t} V_{s,t} \right) \equiv \mathcal{R}_t \\ \Rightarrow B_{t+1} &= (1-\delta)B_t + \mathcal{R}_t - C_t^K, \end{aligned}$$

where  $D_{s,t}$  are the dividends earned from the firms of sectors  $s = 1, \dots, S$ . When  $s \in \mathcal{S}_t$ , this dividend is positive, whereas when  $s \notin \mathcal{S}_t$ , this dividend is negative and equal to  $\kappa_{s,t} V_{s,t}$  for each firm planning to reopen in the next period. The Euler equation defines the discount factor  $\tilde{\beta}_t = \beta_t \left( \frac{C_{t+1}^K}{C_t^K} \right)^{-\nu}$ . In the following, we assume that  $B_t > 0, \forall t$ .<sup>10</sup> This assumption is sustainable, because the pricing of the vacancy costs prior to reopening ( $\psi_s$ ) can be arbitrarily low. The particular assumptions made with regard to the capitalist's preferences drive consumption to be autonomous; this property implies that all the income fluctuations of the capitalist are absorbed by changes to their inventories  $B_{t+1}$ .<sup>11</sup>

<sup>10</sup>Indeed, we must have  $B_t \geq 0, \forall t$ . When this constraint is binding, this implies that the capitalist cannot finance the reopening costs of the firms; this leads them to close, regardless of anticipated profits.

<sup>11</sup>With the solution for the consumption  $C_t^K = \left( \frac{\tilde{\beta}_t A_b}{1-\tilde{\beta}_t(1-\delta)} \right)^{\frac{-1}{\nu}}$ , we have  $B_{t+1} - (1-\delta)B_t = \mathcal{R}_t - C_t^K$ .



### 2.1.2 Financially constrained agents: the workers

Workers are risk-neutral and are characterized by their skill  $q \in \bar{\mathcal{S}}$ . The preferences of each agent  $i$  with the skill  $q$  are defined as follows:

$$C_{i,q,t}^L = S_{n,t}^{\frac{1}{1-\sigma}} \left( \sum_{s \in \mathcal{S}_t} (C_{i,q,s,t}^L)^{\frac{\sigma-1}{\sigma}} \right)^{\frac{\sigma}{\sigma-1}}.$$

Their resource constraint is given by

$$I_{i,q,t} = \sum_{s \in \mathcal{S}_t} p_{s,t} C_{i,q,s,t}^L = C_{i,q,t}^L \quad \text{for} \quad I_{i,q,t} = \{w_{i,q,t}(\alpha), b_{i,q}\} \quad \forall q \in \bar{\mathcal{S}},$$

where  $w_{i,t}(\alpha)$  denotes the real wage of the employed worker and  $b_i$  is the real unemployment benefit of the unemployed worker. The value functions of each worker are

$$\begin{aligned} W_{i,q,t}(\alpha) &= w_{i,q,t}(\alpha) + \tilde{\beta}_t \left[ (1 - s_{q,t+1}) \int_{\alpha_{q,t+1}^r}^{\infty} W_{i,q,t} \frac{dG(\alpha)}{1 - G(\alpha_{q,t+1}^r)} + s_{q,t+1} U_{i,q,t+1} \right] \\ U_{i,q,t} &= b_{i,q} + \tilde{\beta}_t \left[ f_{q,t+1} (1 - s_{q,t+1}) \int_{\alpha_{q,t+1}^r}^{\infty} W_{i,q,t} \frac{dG(\alpha)}{1 - G(\alpha_{q,t+1}^r)} + (1 - f_{q,t+1} (1 - s_{q,t+1})) U_{i,q,t+1} \right], \end{aligned}$$

where  $\tilde{\beta}_t$  is the discount factor,  $s_{q,t}$  the endogenous job-separation rate, and  $f_{q,t}$  the meeting rate between an unemployed job seeker and a vacant job position.

## 2.2 Labor market flows

As in the DMP model, a matching function generates meetings, whereas separations result from the selection of workers that are more productive than an endogenous threshold. The labor market for each skill  $s$ . Workers and firms direct their search efforts in the one corresponding submarket corresponding to a skill  $s \in \bar{\mathcal{S}}$ . Following Den Haan et al. (2000), the matching function for each sector is

$$M_s(U_{s,t}, V_{s,t}) = \frac{U_{s,t} V_{s,t}}{(U_{s,t}^\tau + V_{s,t}^\tau)^{1/\tau}},$$

ensuring that the probabilities of an unemployed worker finding a job per unit of time  $f_s(\theta_{s,t}) = \frac{M(U_{s,t}, V_{s,t})}{U_{s,t}} = (1 + \theta_{s,t}^{-\tau})^{-1/\tau}$  and the vacancy to be filled  $q_s(\theta_{s,t}) = \frac{M(U_{s,t}, V_{s,t})}{V_{s,t}} = (1 + \theta_{s,t}^\tau)^{-1/\tau}$  are in the interval  $[0; 1]$ .

At the beginning of each period  $t$ , the number of workers inside the firm is the sum of the hirings in the previous period ( $q_{s,t-1} V_{s,t-1}$ ) and the previous employment stock ( $N_{s,t-1}$ ).

Then, in each firm  $i$  of sector  $s$ , an idiosyncratic shock takes place and the productivity of worker ( $\alpha_{i,s,t}$ ) is discovered. There are separations if  $\alpha < \alpha_{i,s,t}^r$ . This threshold provides the mass of endogenous separations. Note that the pool of separation includes old and new matches. The microeconomic shock  $\alpha$  is drawn in the time-varying distribution  $G_{s,t}(\alpha)$ , which is a log-normal distribution with a mean  $\mu_G$  and a variation  $\sigma_{s,t}$ . To account for the increase in microeconomic risk in a recession, we assume that

$$\sigma_{s,t} = \sigma_G \left( \frac{U_t}{U} \right)^{\xi_s}, \quad (1)$$

where the current unemployment rate level  $U_t$  and its long-term value  $U$  are taken as given at the level of the firm  $i$  on the labor market segment  $s$ . The parameter  $\xi$  controls the impact of the recession on  $\sigma_t$ .<sup>12</sup> Once the information on productivity is revealed, the stock of employment available for production can be determined; from there, wage-bargaining can occur and, finally, production takes place. It is only at the end of period  $t$  that the stocks of unemployment ( $U_{s,t}$ ) and employment ( $N_{s,t}$ ) are given, allowing one to determine new matches that occur through the choice of  $V_{s,t}$ , based on  $q_{s,t}$ .

The law of motion of employment is

$$N_{s,t} = (1 - s_s)(1 - G_{s,t}(\alpha_{s,t}^r))(N_{s,t-1} + q(\theta_{s,t-1})V_{s,t-1}), \quad (2)$$

where  $0 < s_s < 1$  is the exogenous probability of job destruction. The job-separation rate is defined by  $JSR_t \equiv s_{s,t} = s_s + (1 - s_s)G_{s,t}(\alpha_{s,t}^r)$ , and it gives the INs to unemployment, given the information of the period  $t$ . The job-finding rate is defined by  $JFR_t \equiv f_{s,t} = (1 - s_{s,t+1})f_s(\theta_{s,t})$ , and it gives the OUTs to unemployment, taking into account not only the information of period  $t$  but also that of period  $t + 1$ . Finally, the normalization of the population size to unity leads to  $\varphi \sum_{s=1}^S \omega_s(U_{s,t} + N_{s,t}) + (1 - \varphi) = 1$ .

## 2.3 Firms

For firm  $i$  from sector  $s$ , hirings result from a search process that consists of posting the number of vacancies  $V_{i,s,t}$  that will be matched with unemployed workers with a probability  $q_{s,t}$ ; this is not controlled by the firm. The unit cost, in production units, of each vacancy is given by

$$\kappa_{i,s,t} = \kappa_{s,t} = \kappa_s \left( \frac{U_{s,t}}{U_s} \right)^{\gamma_s} \quad \forall i, \quad (3)$$

---

<sup>12</sup>The countercyclical of firm-level microeconomic risk is documented by Bloom (2009) and Bloom et al. (2018).

where both the current unemployment rate level  $U_{s,t}$  and its long-term value  $U_s$  are taken as given at the level of the firm  $i$  on the labor market segment  $s$ ; this leads one to interpret the time-varying component of the vacancy cost as a congestion externality.<sup>13</sup> Given that  $\gamma_s$  depends on  $s$ , this congestion externality is sector-specific. Unit costs are higher during a recession, because at such a time, each vacant job (which are scarce in such period) receives a very large number of applications (and the number of unemployed individuals is important). Therefore, recessions increase the cost of treatment for each application.<sup>14</sup>

Denoting  $\tilde{\alpha}_{s,t} = \frac{\int_{\alpha_{s,t}^r}^{+\infty} \alpha dG_{s,t}(\alpha)}{1-G_{s,t}(\alpha_{s,t}^r)}$ , the production function is<sup>15</sup>  $Y_{s,t} = A_{s,t}A_t\tilde{\alpha}_{s,t}N_{s,t}$ , where  $A_{s,t}$  and  $A_t$  are the skill-specific and aggregate productivity, respectively. Denoting  $\tilde{w}_{s,t} = \frac{\int_{\alpha_{s,t}^r}^{+\infty} w_{s,t}(\alpha)dG_{s,t}(\alpha)}{1-G_{s,t}(\alpha_{s,t}^r)}$ , the firm's objective is to maximize its discounted profits:

$$\max \sum_{\tau=0}^{+\infty} \tilde{\beta}_t^\tau D_{s,t+\tau} = \max \sum_{\tau=0}^{+\infty} \tilde{\beta}_t^\tau \{p_{s,t+\tau}Y_{s,t+\tau} - \tilde{w}_{s,t+\tau}N_{s,t+\tau} - \kappa_{s,t+\tau}V_{s,t+\tau}\},$$

subject to Equation (2) and the Kuhn–Tucker conditions, given by<sup>16</sup>

$$q_s(\theta_{s,t})V_{s,t} \geq 0, \quad \lambda_{s,t} \geq 0, \quad \text{and} \quad \lambda_{s,t}q_s(\theta_{s,t})V_{s,t} = 0.$$

**Regime 1.** If the expectation of the average job value is sufficiently large to lead  $V_{s,t} > 0$ , then  $\lambda_{s,t} = 0$ . In this case, the dynamics are given by

$$\begin{aligned} 0 &= p_{s,t}A_{s,t}A_t\alpha_{s,t}^r - w_{s,t}(\alpha_{s,t}^r) + \frac{p_{s,t}\kappa_{s,t}}{q(\theta_{s,t})} \\ \frac{p_{s,t}\kappa_{s,t}}{q_s(\theta_{s,t})} &= \tilde{\beta}_t \left[ (1 - s_{s,t+1}) \left( p_{s,t+1}A_{s,t+1}A_{t+1}\tilde{\alpha}_{s,t+1} - \tilde{w}_{s,t+1} + \frac{p_{s,t+1}\kappa_{s,t+1}}{q_s(\theta_{s,t+1})} - \lambda_{s,t+1} \right) \right]. \end{aligned}$$

Note that when the firm cannot sell today (i.e.,  $p_{s,t}$  does not exist) but expects a recovery, it can borrow resources from the capitalist and then restart its activity, even after activity cessation in period  $t$ .

<sup>13</sup>We choose the same functional form as Hall and Kudlyak (2020), but we introduce a sector-specific parameter  $\gamma_s$  that induces a sector-specific congestion externality.

<sup>14</sup>Blanchard and Diamond (1994) were the first to elucidate the foundations of these countercyclical unit costs, based on the existence of exchange externalities: they show that in a labor market where entrepreneurs prefer hiring short-term unemployed workers, recessions lead to an increase in the share of long-term unemployed workers who then congest the hiring process. Hall and Kudlyak (2020) show why this congestion effect matters if the DMP model is to reproduce the observed persistence of unemployment after a recession. Moreover, Engbom (2019) and Molavi (2018) suggest that countercyclical hiring unit costs are supported by the data.

<sup>15</sup>In the following, we omit for simplicity the index  $i$ , which denotes firm  $i$  in each sector  $s$  because the equilibrium is symmetrical within sectors.

<sup>16</sup>See Appendix A for more details on the firm's problem solutions.

**Regime 2.** If the expectation of the average job value is sufficiently low leading to  $V_{s,t} = 0$ , then  $\lambda_{s,t} > 0$ . When  $V_{s,t} = 0$ , we have  $\theta_{s,t} = 0 \Leftrightarrow q(\theta_{s,t}) \rightarrow 1$ . Therefore, the dynamics are given by

$$\begin{aligned} 0 &= p_{s,t}A_{s,t}A_t\alpha_{s,t}^r - w_{s,t}(\alpha_{s,t}^r) + (p_{s,t}\kappa_{s,t} - \lambda_{s,t}) \\ \lambda_{s,t} &= p_{s,t}\kappa_{s,t} - \tilde{\beta}_t \left[ (1 - s_{s,t+1}) \left( p_{s,t+1}A_{s,t+1}A_{t+1}\tilde{\alpha}_{s,t+1} - \tilde{w}_{s,t+1} + \frac{p_{s,t+1}\kappa_{s,t+1}}{q_s(\theta_{s,t+1})} - \lambda_{s,t+1} \right) \right]. \end{aligned}$$

When the solution is constrained at  $\theta_{s,t} = 0$ , then we have  $N_{s,t} = (1 - s_s)(1 - G_{s,t}(\alpha_{s,t}^r))N_{s,t-1}$  until  $\theta_{s,t+n} > 0$  in  $n$  periods. Note that it is possible to reach  $N_{s,t} = 0$  if  $\alpha_{s,t}^r$  leads to  $G_{s,t}(\alpha_{s,t}^r) = 1$ .

## 2.4 Wages

To determine the equilibrium wage, we use a sharing rule of a generalized Nash bargaining process between the worker and the firm where  $\eta_s \in (0, 1)$  is the heterogeneous workers' relative bargaining weight and  $b_s$  is the heterogeneous workers' flow value of unemployment activities. Moreover, as usual in quantitative evaluation of standard DMP models, it is relevant to introduce real wage rigidities<sup>17</sup> — recently reaffirmed by the studies of Kurmann and McEntarfer (2019) and Jardim et al. (2019)<sup>18</sup> and put back in the spotlight by Cortes and Forsythe (2020) using the COVID-19 crisis experience<sup>19</sup>. There are several ways to introduce real wage rigidities in DMP models: (i) an alternating offer bargaining game as in Hall and Milgrom (2008) or (ii) the incorporation of a wage norm or social consensus as in Hall (2005). Following Blanchard and Gali (2010) or Leduc and Liu (2019), we adopt the second modelling strategy, knowing that its implications are quite similar to the first one. Therefore, the real wage is a weighted average of the Nash bargaining wage and the steady state wage:

$$w_{s,t}(\alpha) = \varrho_s [\eta_s(p_{s,t}\alpha A_s A_t + p_{s,t}\kappa_{s,t}\theta_{s,t}) + (1 - \eta_s)b_s] + (1 - \varrho_s)w_s, \quad (4)$$

where the free parameter  $\varrho_s \in [0, 1]$  measures the skill specific wage rigidity, and  $w_s$  the steady-state average wage for each  $s$ -type worker. Following Daly et al. (2012) empirical

<sup>17</sup>See, among others, Blanchard and Gali (2010), Christiano et al. (2016), Leduc and Liu (2019), Nicolas Petrosky and Zhang (2020). These papers show that DSGE models with a labor market  $\tilde{A}$  *la* DMP must introduce real wage rigidities to fit the observed characteristics of the US business cycle.

<sup>18</sup>These studies show that roughly 20% of job stayers experienced nominal wage cuts during the recession, while less than 10% had their earnings frozen. See also the survey of Elsby and Solon (2019).

<sup>19</sup>They show that earnings changes for workers who remain employed during the COVID-19 crisis are not atypical during this time period.

study<sup>20</sup>, we assume that wage rigidity decreases with educational level. Hence, we assume that  $\varrho_s = a_\varrho x + b_\varrho$  where  $a_\varrho < 0$ .

## 2.5 General equilibrium

In the following, we normalize the CPI  $p_t = 1, \forall t$ .

**Demand.** Given that the baskets of consumption and inventories are described by the same constant elasticity substitution functions, the aggregate demand for each sector ( $Y_{s,t}^D$ ) is given by

$$Y_{s,t}^D = p_{s,t}^{-\sigma} \left( \frac{\varphi \sum_{j \in \mathcal{S}_t} \omega_j C_{j,t}^L + (1 - \varphi) (C_t^K + I_t^K)}{S_{n,t}} \right),$$

implying that the aggregate demand is  $Y_t^D = \sum_{s \in \mathcal{S}_t} p_{s,t} Y_{s,t}^D$ .

**Supply.** In each goods market, the aggregate supply  $Y_{s,t}^S$  is given by

$$Y_{s,t}^S = \omega_s (Y_{s,t} - \kappa_{s,t} V_{s,t}),$$

implying that the aggregate supply is  $Y_t^S = \sum_{s \in \mathcal{S}_t} p_{s,t} Y_{s,t}^S$ .

**Equilibrium.** Given that  $Y_{s,t}^D = Y_{s,t}^S \equiv Y_{s,t}^*$  at the equilibrium,  $\forall s$ —which implies  $Y_t^D = Y_t^S \equiv Y_t^*$ —the equilibrium prices are deduced from

$$p_{s,t} = \left( \frac{1}{S_{n,t}} \frac{Y_t^*}{Y_{s,t}^*} \right)^{\frac{1}{\sigma}} \quad \forall s \in \mathcal{S}_t.$$

**Labor market.** Using the wage equation (Equation (4)), we obtain the job-destruction condition (reservation productivity), and the job-creation condition (hirings) by regrouping Equations (10)–(13) of Appendix A:

$$\alpha_{s,t}^r = \max \left\{ 0; \frac{1}{(1 - \eta_s) p_{s,t} A_{s,t} A_t} \left( (1 - \eta_s) b_s + \eta p_{s,t} \kappa_{s,t} \theta_{s,t} - \frac{p_{s,t} \kappa_{s,t}}{q(\theta_{s,t})} - \lambda_{s,t} \right) \right\} \quad (5)$$

$$\frac{p_{s,t} \kappa_{s,t}}{q_s(\theta_{s,t})} - \lambda_{s,t} = \tilde{\beta}_t \left[ (1 - s_{s,t+1}) \left( p_{s,t+1} A_{s,t+1} A_{t+1} \tilde{\alpha}_{s,t+1} - \tilde{w}_{s,t+1} + \frac{p_{s,t+1} \kappa_{s,t+1}}{q_s(\theta_{s,t+1})} - \lambda_{s,t+1} \right) \right] \quad (6)$$

**Closure and reopening of a business sector.** A recession can lead one sector  $s$  to close ( $N_{s,t} = 0$ ) or be unable to sell ( $Y_{s,t} < \kappa_{s,t} V_{s,t}$ ) in period  $t$ . If this be the case, then the number of exchanged varieties is lower than its maximal number (i.e.,  $\dim(\mathcal{S}_t) < S$ ). At

<sup>20</sup>See <https://www.frbsf.org/economic-research/indicators-data/nominal-wage-rigidity/> for updated data until 2020

the same time, however, the entrepreneur’s expectations can lead them to reopen in  $t + 1$ . Therefore, it is necessary to borrow in  $t$  from the capitalist an amount of their storable goods to post vacancies at period  $t$  in order to restart the activity in  $t + 1$ . Given that this sector  $s$  has a “negative” net supply ( $Y_{s,t}^S = \omega_s (Y_{s,t} - \kappa_{s,t} V_{s,t}) < 0$ ), there are no sales for sector  $s$  in period  $t$ . Without any information on the relative price of these goods  $s$  in  $t$ , this transaction is valued at the price  $\psi_s$  in the budget constraint of the capitalist.<sup>21</sup> If the capitalist does not exist, firms cannot reopen after a period without sales.

### 3 Calibration based on the subprime crisis experience

In this section we present our calibration strategy. We use worker flows by education level and the major features of the 2008 subprime crisis. This allows us to identify the parameters allowing our model to explain a crisis driven by a common shock on each labor market segment.

#### 3.1 Parameters based on external information

The model is calibrated at a monthly rate. Thus, the average value for  $\tilde{\beta}_t = 1/(1 + 0.0573)^{1/12}$ .<sup>22</sup> For the capitalist’s preference parameters, we set  $\delta = 0.025/12$  following Harding et al. (2007); we also set  $\nu = 1.7$ , which is in the range of the estimation of Attanasio and Vissing-Jorgensen (2003). We calibrate the share of this population to represent 2% of the overall population, with a saving rate of 10% (See Saez and Zucman (2014)). This allows us to deduce the steady-state values for  $C^K$  and  $B^K$  and identify  $A_b$ .

For the workers, we normalize the average of the aggregate productivity component to unity ( $A = 1$ ). Each “sector” represents the production of a worker type, which is identified by their educational attainment.<sup>23</sup> We restrict the log-normal distributions of  $\alpha$  to be the same for each subpopulation, with a zero mean and a standard deviation equal to 0.12, as in Krause and Lubik (2007).

---

<sup>21</sup>This shadow price  $\psi_s$  is calibrated such that the storable goods of the capitalist always respect  $B_t > 0$ .

<sup>22</sup>This value matches the mean discount rate in international data, which is 5.37% per annum.

<sup>23</sup>As this characteristic practically does not change after entering the labor market, this segmentation justifies the absence of mobility between “sectors” assumed in our model.

### 3.2 Parameters based on first-order moments restrictions

Using data from Cairo and Cajner (2016), we derive worker flows based on Current Population Survey (CPS) data (January 1976–January 2014). To use a larger sample, we rescale these data to be coherent with aggregate worker flows calculated from US Bureau of Labor Statistics (BLS) data (1947–2020).<sup>24</sup> The first-order moments of worker flows used to identify the model parameters are shown in Table 1, where all job-finding rates ( $JFR$ ) are the same, as they are not significantly different from the average. At the steady state, these moments are linked by the restrictions  $UR_s = \frac{JSR_s}{JSR_s + JFR_s}$ . Assuming,

	LHS	HS	Coll.	Bach.	Aggregate
$JFR$	0.411	0.411	0.411	0.411	0.411
$JSR$	0.052	0.029	0.024	0.019	0.024
$UR$	0.112	0.066	0.055	0.030	0.057
Population shares	8.984%	28.626%	35.406%	26.982%	100%

Table 1: **Worker flows and stocks.** Data came from Cairo and Cajner (2016) and cover the 1976–2014 period; we rescaled these data. For population shares, the data came from the BLS and cover the 2000–2020 period. The educational attainment typologies are as follows: less than high school diploma (LHS), high school diploma (HS), college diploma (Coll.) and bachelor degree or more (Bach.).

	LHS	HS	Coll.	Bach.
$s_s^{endo}$	0.0172	0.0095	0.0079	0.0041
$s_s^{exo}$	0.0353	0.0198	0.0165	0.0087
$\tilde{\alpha}_s$	1.0119	1.0099	1.0095	1.0085
$\eta_s$	0.4234	0.4841	0.4992	0.5406
$rb_s$	0.9577	0.9508	0.9487	0.9417

Table 2: **Results of the calibration using labor market restrictions.**

as in Den Haan et al. (2000) or Krause and Lubik (2007), that 68% of the separations are exogenous, the job-separation rates by skill ( $JSR_s$ ) give the equilibrium values of the productivity reservation threshold ( $\alpha_s^r$ ). Using the job-finding rates by skill ( $JFR_s$ ), we deduce the equilibrium value of the skill specific unemployment rate ( $\theta_s$ ). Applying the definitions of the skill specific unemployment rate ( $UR_s$ ), we can then deduce vacancies ( $V_s$ ) at the steady state. Finally, with the log-normal distribution of  $\alpha$ , we deduce the

<sup>24</sup>See Appendix B for more details on the data.

mean productivity of each skill ( $\tilde{\alpha}_s$ ). Using Equations (5)–(6) taken at the steady state and assuming that  $\kappa_s$  is proportional to  $A_s$ , s.t.  $\kappa_s = kA_s$ , we identify  $\eta_s$  and  $\tilde{b}_s \equiv b_s/(p_s A_s)$ , which are thus skill-specific. The value of  $k$  is chosen such that the average bargaining power over all skills is equal to 1/2.<sup>25</sup> The results of this calibration procedure are reported in Table 2.

Moreover, we restrict the set of parameters to minimize the distance between the skill-specific relative wage in the model and its empirical counterpart.<sup>26</sup> Hence we restrict the values of  $\{A_s\}_{s=1}^S$  such that the model matches the average wages by education level, as observed in the United States:

$$\frac{w_s^{data}}{\text{mean}(w_s^{data})} = \frac{p_s A_s \Gamma_s}{\sum_{s=1}^S \tilde{\omega}_s p_s A_s \Gamma_s} \quad \text{with } \Gamma_s = \eta_s(\tilde{\alpha}_s + k\theta_s) + (1 - \eta_s)\tilde{b}_s,$$

where empirical data are denoted as  $w_s^{data}$ . Nevertheless, this restriction depends on the equilibrium prices  $p_s$ . Therefore, this identifying system is solved using all the general equilibrium restrictions:

$$p_s = \left( \frac{1}{S} \frac{\sum_{s=1}^S p_s \omega_s (Y_s - \kappa_s V_s)}{\omega_s (Y_s - \kappa_s V_s)} \right)^{\frac{1}{\sigma}} \quad \text{with } Y_{s,t} = A_s N_s \tilde{\alpha}_s,$$

which give the consistent relative prices  $p_s$ ,  $\forall s$ . This procedure obtains a unique solution if we add the normalization  $\sum_s \omega_s p_s A_s = 1$  (i.e., the average productivity is equal to unity).

### 3.3 Parameters based on out-of-steady state model implications

To generate a financial crisis, we introduce a common financial shock—which is to say, one that strikes all economic players uniformly—to reproduce the depression and recovery observed in the US labor market. Following Hall (2017), we model this financial shock as

---

<sup>25</sup>See Appendix C for more details.

<sup>26</sup>The wage statistics derive from weekly and hourly earnings data from the CPS, over the 2000 Q1 to 2020 Q1 period.



a drop in the discount rate, as if this rate included variations in the risk premium.<sup>27,28</sup> Given that the DMP model is an asset-pricing model, expectations in the risk premium are important for valuating jobs, and so they have a direct impact on hiring and separation decisions. By reducing the discount factor, the financial crisis reduces the discounted value of expected profits, then instantaneously reduces (increases) hirings (separations). We assume that the sequence of  $\beta_t$  is given by the following process:

$$\beta_t = \rho_b \beta_{t-1} + (1 - \rho_b) \beta - \frac{\epsilon_{b,0}}{\vartheta_b^{(t/\mu_b)}},$$

where  $\rho_b$  gives the persistence of the AR part of the process,  $\epsilon_{b,0}$  the initial size of shock, and  $\vartheta_b^{(t/\mu_b)}$  the chronic property of the shocks as a function of  $\epsilon_{b,0}$ . To identify the remaining parameters

$$\Psi = \{\sigma, \tau, \{\xi\}_{s=1}^S, \{\gamma_s\}_{s=1}^S, a_\varrho, b_\varrho, \rho_\beta, \epsilon_{\beta,0}, \vartheta_\beta, \mu_\beta\},$$

with  $\dim(\Psi) = 8 + 2 \times S$  and  $S = 4$ , we choose moments that describe the worker flows during the 2008 subprime crisis (i.e., the most recent crisis, prior to COVID-19). This allows the model to reveal under which restrictions it can generate a deep crisis.<sup>29</sup>

We identify  $\Psi$  using

$$\Phi = \left\{ \left\{ JSR_{s,t} \right\}_{t=t_0}^{t_1}, \left\{ JFR_{s,t} \right\}_{t=t_0}^{t_1} \right\}_{s=1}^S,$$

where  $t_0$  corresponds to September 2008 and  $t_1$  to December 2013. Given that  $\dim(\Phi) = 64 \times 4 \times 2 = 512 > \dim(\Psi) = 16$ , this strategy can be interpreted as an informal test

---

<sup>27</sup>Indeed, the risk premium data exhibited a prominent spike in 2008–2009, when it exceeded its historical average during this Great Recession: the difference between the yield on a risky bond (given by the 5-Year High Quality Market (HQM) Corporate Bond Spot Rate) and the yield on a Treasury bond of equivalent maturity rose from 0.6 points in January 2007 to 5.45 points in October 2008. In 2008, the expectations of an increase in risk led to an increase in the risk premium and thus induced a drop in the discount factor. Since the risk premium measures expectations of credit risk and default in the economy, it serves as an important measure by which to monitor markets and ascertain whether a downturn is expected in the near future.

<sup>28</sup>In Martellini et al. (2020), a discount rate decrease- by reducing the expected profits- cuts incentives to open vacancies, but also the job-to-job mobilities and thus job separations, given that agents can search on-the-job. Hence, the impact of discount rate changes on unemployment is ambiguous. This is not the case in our model where the reduction of the expected profits cuts the job finding rates and rises job separation rates leading unambiguously to unemployment increases.

<sup>29</sup>We assume that the economy is initially at the steady state. At date  $t_0$ , the aggregate shock makes the economy deviate from its steady path. At the final date  $t_*$ , the economy converges back to its steady state. We set  $T = t_* - t_0 = 120$ , which means that 10 years after the shock, the economy has reverted to its steady state.

of the model.<sup>30</sup> We search  $\Psi$ , which minimizes the root mean square error for each time series in  $\Phi$ . Table 3 reports the value of the identified parameters.

Common Parameters		$\sigma$	$\tau$	$a_\varrho$	$b_\varrho$
		2	1.5	-0.14	0.57
		$\rho_b$	$\epsilon_{b,0}$	$\vartheta_b$	$\mu_b$
		0.1	0.085	1.17	2.6
		LHS	HS	Coll.	Bach.
Specific Parameters	$A_s$	0.48	3.07	5.21	8.27
	$\xi_s$	0.6	0.55	0.5	0.35
	$\gamma_s$	0.9	0.6	0.5	0.3
Equilibrium values	$p_s$	4.95	1.07	0.74	0.66
	$p_s A_s$	2.40	3.30	3.85	5.47
	$\frac{w_s}{\sum_s \omega_s w_s}$	0.60	0.82	0.96	1.36

Table 3: **Results of the calibration.**

With these parameters, our model appears to reproduce the magnitude and persistence of the impact of this crisis, as well as these contrasted impacts on heterogeneous workers (see the Figures in Appendix D). The peak in unemployment for those with a diploma lower than those issued in high schools saw a five points increase in the unemployment rate compared to the 2008 summer level. This increase was by only 3.5 points for those who graduated from a high school, 3 points for those with a diploma issued by a college, and 1.5 points for those having a bachelor degree or more. The model succeeds in reproducing this heterogeneity on the labor market. Consistent with the work of Cairo and Cajner (2016), these differences in the adjustment of unemployment rates are due to the greater amplitudes of separations according to educational attainment: less-educated graduates lose their jobs more easily than more-educated ones, while for all types of graduates the chances of finding a job decrease in the same proportions. Therefore, endogenous separations are crucial for explaining heterogeneity in unemployment dynamics.

Despite the absence of persistence of microeconomic shocks, our model extends beyond the usual limits of the DMP model by generating a large endogenous persistence: unemployment reverts to its initial value after seven years.

Hence, our model appears to reproduce the magnitude and the persistence of a crisis, as

<sup>30</sup>In accordance with the model where the participation rate is constant and mobility across submarket is nil, the job finding and separation rates ( $JFR_{s,t}$ ,  $JSR_{s,t}$ ) give the unemployment rate ( $UR_{s,t}$ ),  $\forall s, t$ .

well as the contrasted impacts on heterogeneous workers. For these reasons, this model can be used to predict economic fallout dovetailing from the COVID-19 crisis.

## 4 Explaining the impact of COVID-19

We model the lockdown by two exogenous changes in the parameters. First, we consider that the restrictions on transactions induced by the lockdown are as if the TFP has been reduced. Secondly, we assume that the CARES act reduces the costs of re-employing workers after a separation. Indeed, the Paycheck Protection Program (PPP) of the CARES act allow firms to reimburse their loans if they maintain their precrisis level of full-time equivalent employees.<sup>31</sup> More formally, we assume that the unit cost of a vacancy is

$$\tilde{\kappa}_{s,t} = (1 - (1 - \varsigma \times t)\varpi_s)\kappa_{s,t} \quad \text{for } t \in [\tilde{t}_0, \tilde{t}_1] \text{ with } \begin{cases} \tilde{t}_0 = 0 & \text{in April 2020} \\ \tilde{t}_1 = 7 & \text{in November 2020} \end{cases}$$

where  $\varpi_s$  is the initial drop in hiring cost and  $\varsigma$  the speed decrease in cost reductions. These shocks on hiring costs induced by policy responses to pandemic crisis generated by the lockdown are necessary because, as Figure 2 shows, the composition of separations between temporary and not temporary job losers has highly changed between the two last crises: during the COVID-19 crisis, the larger share of temporary separations suggest that the recall option is more used, then reducing the hiring costs during the recovery.<sup>32</sup>

The empirical studies of Adams-Prassl et al. (2020) and Fana et al. (2020) have also shown that the lockdown measures have unequal impacts on workers. This suggests that the lockdown shocks are worker–skill specific. Assuming that the structure of the US economy has not changed, we use our model, calibrated on subprime crisis, to reveal the monthly sequences of shocks that has hit each type of job since March 2020. We find these sequences of skill-specific shocks by minimizing the distance between data and simulated

---

<sup>31</sup>Borrowers can reimburse their loans corresponding to their expenditures on payroll, rent, utilities, and mortgage interest in the eight weeks after loan receipt, if the borrower maintains their precrisis level of full-time equivalent employees. Otherwise, the amount forgiven falls in proportion to the headcount reduction (payroll expenses must account for at least 75% of the forgiven amount). Therefore, the loan becomes a subsidy if covered operating costs exceed the loan amount and the borrower maintains headcount. See Baker et al. (2020) for more details.

<sup>32</sup>This point has been already suggested by Gregory et al. (2020) and supported by empirical analysis provided by Chodorow-Reich and Coglianesse (2020).

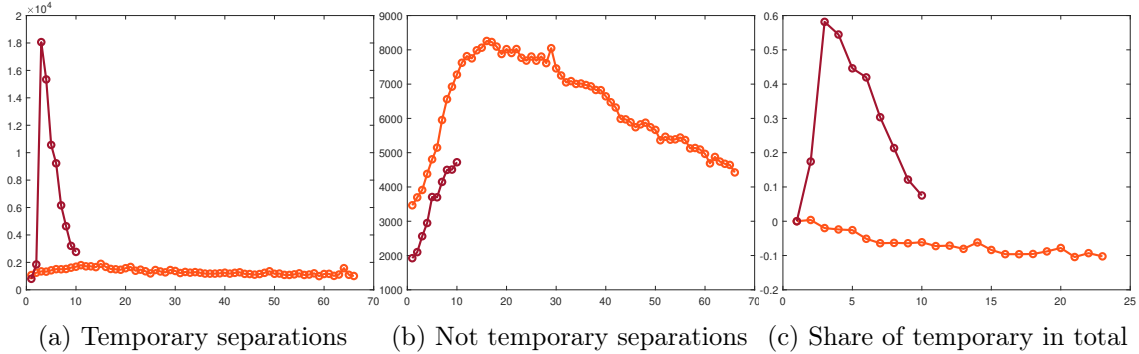


Figure 3: **Separations: temporary vs. not temporary job losers.**

data. Hence, we aim at identifying the following parameters

$$\Gamma = \{ \{A_{s,t}\}_{t=t_0}^{t_1}, \varpi_s, \varsigma \}_{s=1}^S \quad \text{with } t_0 = \text{March 2020 and } t_1 = \text{November 2020}$$

that allow the model to match the following moments:

$$\Upsilon = \{ \{UR_{s,t}\}_{s=1}^{S-1}, JFR_t, JSR_t \}_{t=t_0}^{t_1}.$$

Given that  $\dim(\Upsilon) = 9 \times 5 = 45 > \dim(\Gamma) = 9 \times 4 + 5 = 41$ , this strategy can be interpreted as an informal test of the model. Beyond revealing the unequal impact of the lockdown shocks on each specific occupation, we can also use the model to predict the persistence of the crisis and its consequences in terms of earning losses for each worker type.

## 4.1 Explaining unemployment during the pandemic crisis

**Identifying COVID-19 shocks.** Figure 6 shows the sequences of shocks that allow the model to match the disaggregate unemployment rate, as well as the aggregate job-finding and separation rates ( $\Upsilon$ ). This figure highlights the large unequal impact of lockdown measures, as suggested by Adams-Prassl et al. (2020) and Fana et al. (2020).

In March 2020, the lockdown measures had a negative but moderate impact, estimated between -1.25% and -2.85% of TFP. In April, the impact of the lockdown was much greater, and very unequal. For those with less than a high school diploma, the lockdown reduced workers' productivity by almost 30%, while those who hold a bachelor degree or more saw their productivity decrease by only 3%; for the two other workers types, the negative impact of the lockdown on TFP were between these two extremes (i.e., -23% for those with a high school diploma and -18% for those with a college diploma).

		Mar.	Apr.	May	Jun	Jul.	Aug.	Sep.	Oct.	Nov.	Dec.
LHS	TFP	-2.85	-28.5	-1.9	0	0	0	0	0	0	0
	HC	0	13.5	11.6	9.7	7.8	5.9	4.0	2.2	0.3	0
HS	TFP	-2.25	-22.95	-4.5	0	0	0	0	0	0	0
	HC	0	12.0	10.3	8.6	7.0	5.3	3.6	1.9	0.2	0
Coll.	TFP	-2	-18	-1.2	0	0	0	0	0	0	0
	HC	0	10.5	9.0	7.6	6.1	4.6	3.1	1.7	0.2	0
Bach.	TFP	-1.25	-3	0	0	0	0	0	0	0	0
	HC	0	6.7	5.8	4.9	3.9	3.0	2.0	1.1	0.1	0

Table 4: **Productivity (TFP) and Hiring Costs (HC) reductions  $\forall s, t$  in %** The TFP losses are  $100 \times (A_{s,t} - A_s)/A_s$ , whereas the HC reductions are  $100 \times (1 - (1 - \varsigma \times t)\varpi_s)$ .

Subsequently—which is to say, from June, the month in which the lockdown ended—productivity returned to its precrisis levels, suggesting that economic efficiency is no longer reduced by these restrictive measures.

For the hiring costs, the estimated impact of the CARES act are reductions from 13.5% for the Less than High School workers to 6.7% for those with a Bachelor and more. These cost reductions linearly decline at the same speed for all workers until becoming nil in November 2020.

**Model fit.** Figure 4 shows that (i) data already includes a turning point and (ii) the recovery observed after this date is, at this time, largely more rapid than those seen in previous crises. This suggests that the shock was brutal, and stronger than that seen in previous crises. But, the smaller persistence suggests that the large incentives for temporary separations offered by the CARES act have change the hiring behaviors.

*Unemployment peak.* With calibrated shocks of Table 4, the model reproduces the 12-percentage-point increase in US unemployment (see Panel (c) of Figure 4). The shock sequences that allow the model to match the disaggregated unemployment rates must hit workers unequally (see Table 4), because the increase in unemployment rate among those with less than a high school diploma was by 15.23 percentage points, whereas for those with a bachelor degree or more was by only 6.4 percentage points (see Figure 5). This sharp rise in unemployment is largely due to the impressive drop in hiring (see Panel (a) of Figure 4). However, without the very sharp rise in layoffs (see Panel (b) of Figure 4), the steep increase in the unemployment rate between March and April would not have been possible. Panel (d) of Figure 4 shows the contributions of separations and

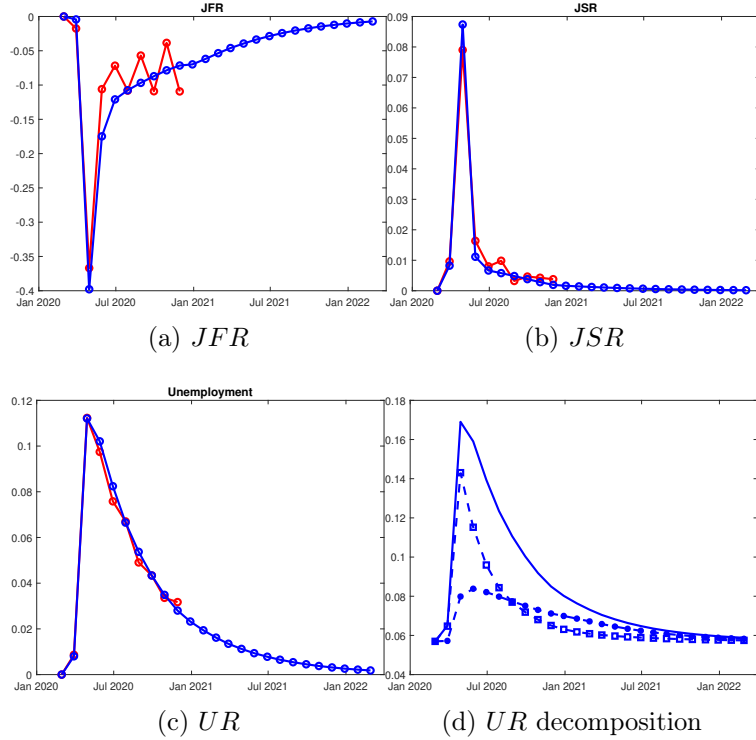


Figure 4: **Aggregate outcomes.** Panels (a)–(c). Red lines: data; Blue lines: model. Panel (d). Line: benchmark case; Dotted line with circles: unemployment rates when  $JSR$  are at their steady-state levels; Dotted line with squares: unemployment rates when  $JFR$  are at their steady-state levels.

findings in unemployment dynamics. The initial increase in unemployment is mainly due to separations (82% of the initial jump in the unemployment rate); however, after three months, unemployment rate adjustments are driven by the job-finding rate.<sup>33</sup>

*Unemployment persistence.* The rapid decline in unemployment is observed for all worker types: in the four labor markets, the fall in unemployment in June had already absorbed half of the increase recorded in April, at the peak of the crisis. Despite the strong recovery observed after April 2020, panel (b) of Figure 4 shows that the separation level still exceeds the February one, which is also matched by the model. This very strong recovery therefore thus requires a very sudden shock sequence for some submarkets, but very little persistence for all. This explains the shapes of the TFP drops reported in Table 4. At the same time, the high speed of unemployment decline, which has never been observed in the previous crisis, requires a significant decline of the congestion costs in the hiring process, thus, leading to the costs reductions reported in Table 4 that will allows the model to match a lower unemployment persistence compared to the previous crises. This also gives the

<sup>33</sup>See Appendix E for more details on labor market indicators by education level.

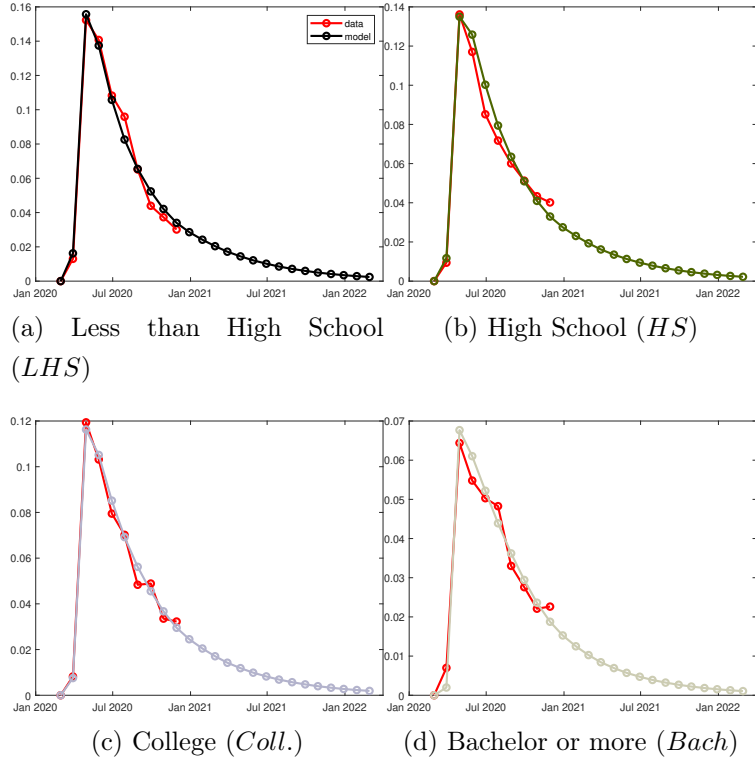


Figure 5: **Disaggregate unemployment rate.**

estimated cuts in unit hiring costs induced by the CARES act.

**Equilibrium adjustments: prices and quantities.** The TFP and HC reductions reported in Table 4 are in units of output of each sector. However, what matters for decisions is the real values of these changes, ie.  $p_{s,t}A_{s,t}$  and  $p_{s,t}\kappa_{s,t}$  not simply  $A_{s,t}$  and  $\kappa_{s,t}$ . Therefore, the prices adjustments  $p_{s,t}$  induced by general equilibrium must be taken into account. Panel (a) of Figure 6 shows that prices of all goods increase due to TFP losses, except for the sector where TFP value is the highest (the ones employing workers with a Bachelor degree or more): in April, the price changes are +14.4% for the goods produced by LHS workers, +7% for those produced by HS workers, +2% for those produced by Coll. workers, but -7% for those produced by Bach. workers. The prices increase mitigates the negative impact of the reductions in TFP (modeling the restrictions on sales) and therefore explains that the most important impact of the crisis is ultimately on the marginal revenues of firms employing High schoolers and College degree workers (see panel (b) in Figure 6). For hiring costs, our calibration revealed that the least educated were victims of greater congestion effect ( $\gamma_s$  decreasing with the level of education). Thus, for the same increase in unemployment, it is those with a low educational attainment who see their

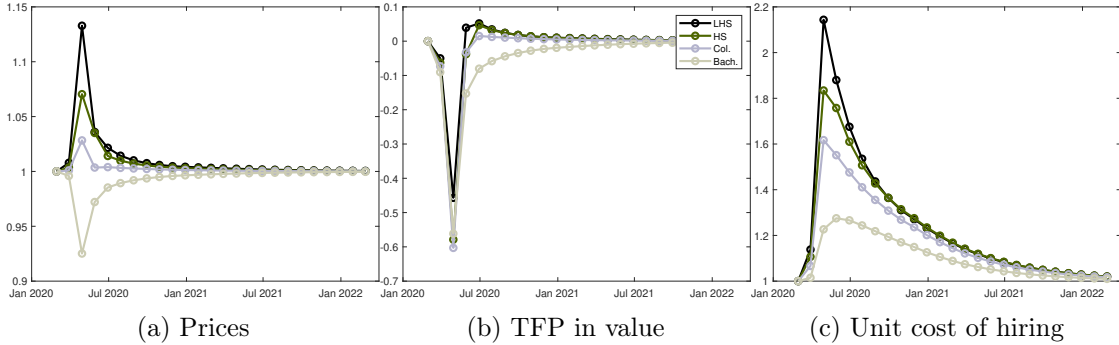


Figure 6: **Equilibrium impact of COVID-19 shocks for each occupation.** Panel (a): price changes  $p_{s,t}/p_s$ . Panel (b): TFP losses in real values in % ie.  $(p_{s,t}A_{s,t} - p_sA_s)/p_sA_s$ . Panel (c): changes in unit costs of hiring, in real values, ie.  $p_{s,t}(1 - (1 - \varsigma \times t)\varpi_s)\kappa_{s,t}/(p_s\kappa_s)$ .

hiring costs in units of goods increase the most. These first adjustments in  $\kappa_{s,t}$  are amplified by the price adjustments: the unit costs of hiring in real value are therefore higher for those with a low level of education after a hard recession (see panel (c) in Figure 6). The impact of the CARES act on these dynamics is to moderate these rises in hiring costs, in particular for the less educated workers (see Table 4).

**Disentangling impact of hiring cost reduction.** Figure 7 shows that without hiring cost reductions, the labor hoarding value is larger and thus the increases in separations and hence in unemployment would have been smaller.

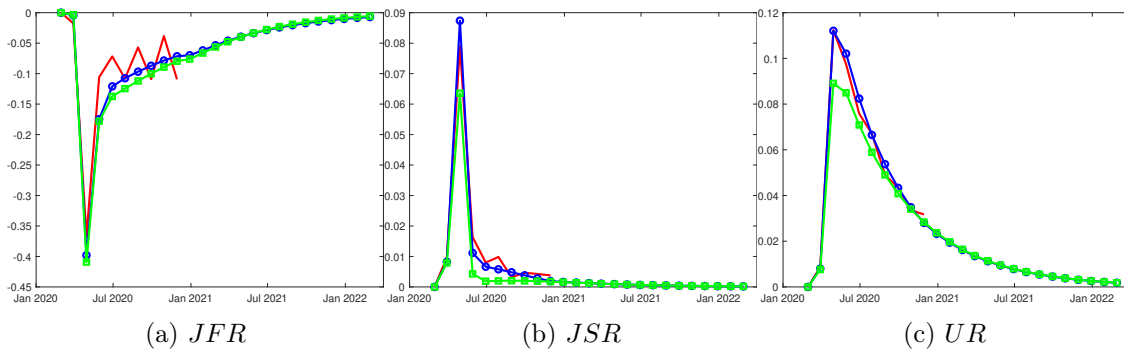


Figure 7: **Aggregate outcomes.** Panels (a)–(c). Red lines: data; Blue lines: benchmark model. Green lines: model without hiring cost reductions.

Therefore, the first impact of the hiring cost reduction that accounts for the CARES act is to increase unemployment by facilitating separations. Given that the CARES act lasts after April, it also induces a persistent increase in separations that would not



occurred without this program. Hence, the inducement of temporary layoffs allowed by CARES act explains 32% of total separations from March to November<sup>34</sup>. Table 5 shows that the CARES act makes it possible to significantly reduce the average duration of unemployment (from more than 3 weeks in April to 1 week in June), which was one of its priority objectives.

	Mar.	Apr.	May	Jun	Jul.	Aug.	Sep.
$\Delta$ Dur. Unemp.	3.2	1.5	1.3	1	0.8	0.6	0.4

Table 5: **Hiring costs reductions and unemployment duration in weeks.**  $\Delta$  Dur. Unemp.: Difference between unemployment duration in the benchmark model and those in model without hiring costs reductions.

**Earning losses.** It seems to us that calculations of the wages lost on account of the pandemic can take two forms. The first is based on the workers' value functions and consists in calculating the cost of the crisis as permanent wage losses that would have been perceived in the absence of a crisis. However, it is well known that this calculation leads to a very low estimate of the costs of a crisis, because the time duration of a crisis represents only a very small fraction of the time of an agent with an infinite life-horizon.<sup>35</sup> The second method focuses more on the short term and consists in measuring wage losses over finite horizons (i.e., first 3 months,..., until the first 24 months after the start of the crisis). In the absence of any information regarding the recurrence of pandemic crises, we favor this latter approach. Therefore, we calculate the transfer, making it possible to compensate for wage losses, with the reference wage being that before the crisis (i.e., the stationary state).<sup>36</sup> Figure 8 shows the wage losses by horizon. Obviously, the longer the horizon is, the smaller the losses will be; in this way, individuals benefit from longer recovery periods. A regularity emerges from Figure 8: the lower the education level is,

<sup>34</sup>These results from our model are supported by the empirical analysis of Bick and Blandin (2020). Based on the Real-Time Population Survey, they show that the share of unemployed workers who expect that they could return to their employers from February, if the conditions improved rapidly, are between 50% and 35%.

<sup>35</sup>This calculation does not bias the evaluation of crises if one takes into account their recurrences and therefore their multiple appearances during an agent's infinite lifetime.

<sup>36</sup>In practice, we calculate the average monthly wage on a horizon  $T$  (i.e.,  $\frac{1}{T} \sum_{t=0}^T w_{s,t} N_{s,t}$ , which we compare to what would have been perceived in the absence of crisis  $w_s N_s$ ). The wage loss is then  $\mathcal{L}_w = \left( \frac{1}{T} \sum_{t=0}^T w_{s,t} N_{s,t} - w_s N_s \right) / N_s$ , or  $\Delta_w = \mathcal{L}_w / w_s$  in percentage. The division by  $N_s$  indicates that the reference population is that before the crisis (i.e., the steady state here); this population is able to evolve within the crisis, as can the chances of being employed.

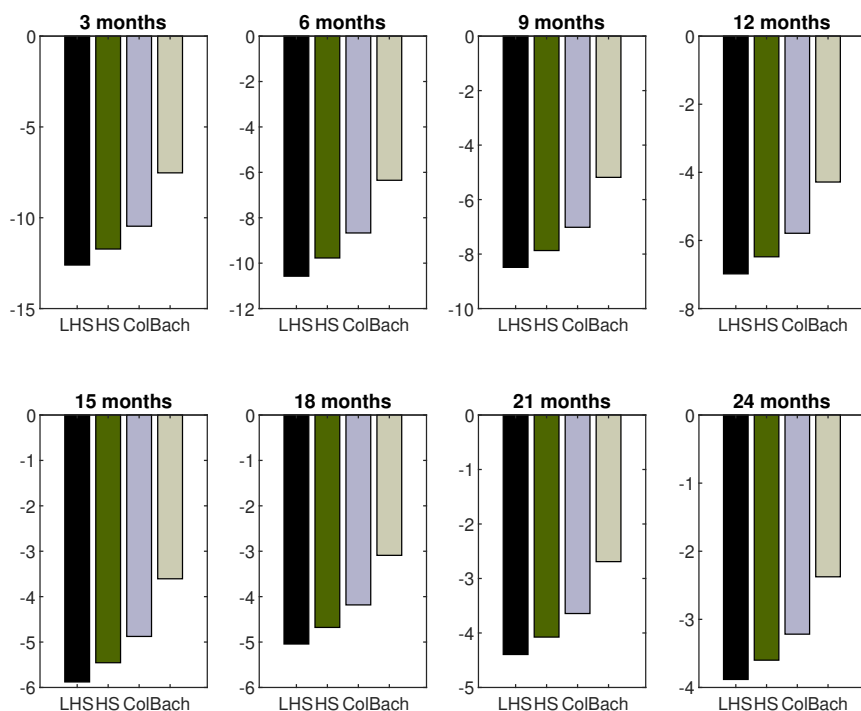


Figure 8: **Wage losses as function of the horizon.**

the greater the loss of wages will be, irrespective of horizon. These wage losses have two causes—namely, variations in the wages of those who are employed, and changes in the chances of being employed. In the model, salary variations compared to the precrisis period do not exceed 5.3%,<sup>37</sup> while variations in employment rates (i.e., the chance of having a job) can drop by 15%. If we look at the period from March to September 2020, the wage losses amount to 12% for workers with less than a high school diploma; for those with at least a bachelor degree, however, that number is 6.9%. Labor income inequalities were already high before the crisis, and it appears that this COVID-19 crisis will only exacerbate them, even if the effect measured here is only transitory.

## 4.2 Contributions of each extension

In this section, we analyze the contribution of (i) the *hiring cost* function that accounts for congestion effects varying with the unemployment; (ii) *real-wage rigidity*, which reduces the response of wages with respect to a wage-setting rule based on the Nash bargain-

<sup>37</sup>In the DMP model, only a fraction of the salary is variable over the business cycle; the portion associated with unemployment benefits is fixed. In addition, in the variable part, productivity and hiring costs that tend to reduce wages in times of crisis are partially offset by the greater selectivity linked to endogenous destruction.

ing solution; and (iii) *varying risk*, which accounts for the increase in microeconomic uncertainty in recession. We then shut off one of these extensions and recalibrate the

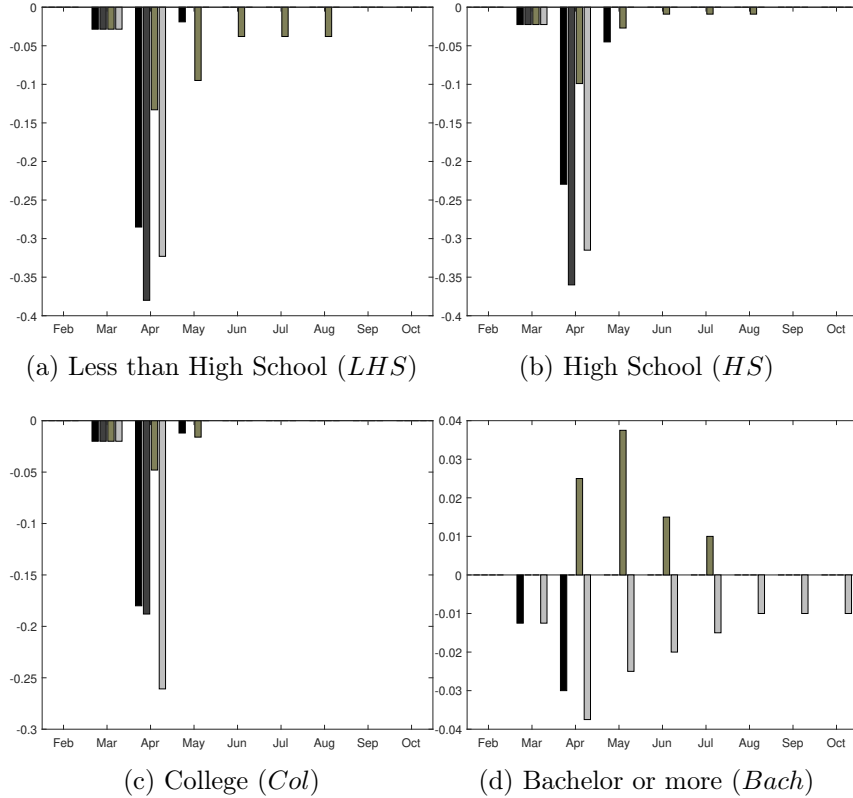


Figure 9: **TFP changes.** Black: Benchmark model. Dark gray: Model without wage rigidity. Khaki: Model without congestion effect on hiring costs. Gray: Model without microeconomic uncertainty. For each scenario, each bar reports the gap relative to the steady-state values.

$T \times S = 36$ -specific shocks, thus allowing the model to match the 36 unemployment rates moments by education level, observed from March to November 2020. We assume that the reductions in hiring costs induced by CARES act are the same than in the benchmark model. Figure 9 reports the estimated sequences of the productivity shocks.<sup>38</sup> For March 2020, the identified shocks all remain the same, irrespective of the model; this can be attributed to the small impact of the crisis during that month. For April and later on, the shocks identification largely depends on model, emphasizing the importance of each extension introduced in the basic DMP model. When the hiring costs are constant—as in the basic DMP model—then the amplitude of the shocks must be smaller, irrespective of education level. However, they must be more persistent: indeed, without the externality

<sup>38</sup>Appendix F provides the exact number for new calibrated values of  $A_{s,t}$ , whereas Appendix G provides the model fits of  $UR$  by skill for the alternative scenarios.

on hiring cost, the internal persistence of the DMP model is very low and must therefore be “replaced” by negative shocks over a greater number of periods, so that the model reproduces the observed data. The absence of wage rigidity or a constant microeconomic risk (which is countercyclical in our benchmark model) drives the estimated shocks to become larger than those in our benchmark model, especially for workers with a high school or college diploma. This finding highlights the fact that these two extensions increase the basic DMP model’s sensitivity to the economic cycle.

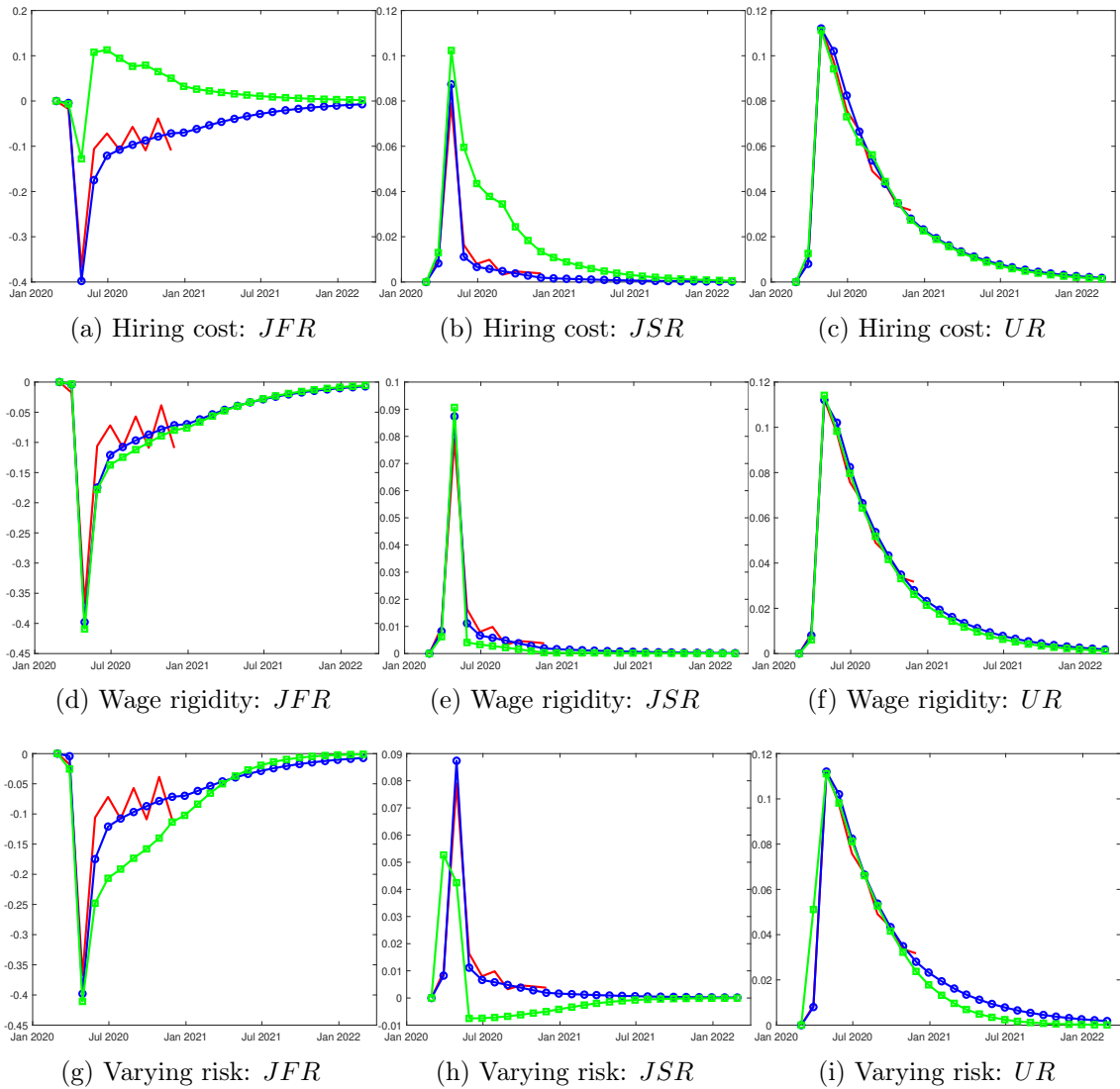


Figure 10: **Aggregate outcomes.** Red lines: data; Blue lines: benchmark model; Green lines: constrained models. “Hiring cost”: results with  $\gamma_s = 0$ ; “Wage rigidity”: results with  $\varrho_i = 1$ ; “Varying risk”: results with  $\xi = 0$ .

One can also determine the importance of each of the aforementioned extensions by mea-

asuring gaps relative to overidentifying conditions. Indeed, our calibration strategy constraints the model to match the monthly unemployment rate by diploma but leaves free the worker flows ( $JFR$  and  $JSR$ ) observed at the aggregate level from March to November 2020. The large differences between the constrained models and the  $JFR$  and  $JSR$  data show that each extension makes a significant contribution (see Figure 10).

When the externality in the hiring cost is suppressed, we re-encounter the usual drawback of the DMP model: the persistence in the job-finding rate below its precrisis value is largely underestimated (Panel (a) of Figure 10): without congestion externality on unit hiring costs, the larger number of unemployed workers in a recession facilitates hiring. To counterbalance this shortcoming, the negative TFP changes for LHS, HS and Coll. workers needed to mimic unemployment rates are more persistent, and thus lead to an overestimation of the job-separation rates (Panel (b) of Figure 10). At the end of lockdown, it is also necessary to introduce TFP increases for jobs held by graduates of a bachelor's degree or more, which is counterfactual.

When the wage rigidity is removed, TFP changes are strongly persistent in order to compensate for the lack of internal persistence. Despite this over-estimated persistence of shocks, the persistence in  $JSR$  is lower than in the benchmark model (Panel (e) of Figure 10). This shortcoming comes from persistent wages below their precrisis levels, which prevents firms from firing workers after the months where shocks are negative. The discrepancy between the model and the data is even more larger when the hiring cost reductions (CARES act effect) are removed simultaneously with wage rigidity. In this case, the job-separation rates fall below their steady-state level three months after the start of the crisis (see panel (a) of the Figure 17 in Appendix H). This is at odds with the data.

When the time-varying risk of microeconomic shocks is removed ( $\sigma_{s,t} = \sigma_G, \forall s, t$ ), both the  $JSR$  and  $JFR$  are biased, despite the good fit of unemployment. During a recession, the increase in  $\sigma_{s,t}$  (with the average of the distribution remaining constant) expands the weight of both excellent and very bad draws. Since the distribution that matters for evaluating expected profits is cut to the left by reservation productivity, an increase in variance raises the expected profits, which in turn boosts hires. Panel (g) of Figure 10 shows that without this effect, the expected profits would be lower, which would lead to fewer hires. For separations, this effect also acts to reduce  $JSR$ , but it is overcompensated by (i) the increase in labor market tightness, which increases wages, and (ii) the thickening of the left-tail distribution, which pushes up the mass of firings. Hence, an increase in the variance of the distribution implies an increase in the mass of low-productive jobs

at the profitability limit.<sup>39</sup> Therefore, in the absence of this effect, there would be less separations (see Panel (h) of Figure 10).

### 4.3 Alternative scenarios: longer but less stricter lockdown

What would happen if we had less stricter lockdown but a more persistent one? In order to control that only, the lockdown duration changes. TFP changes are calibrated so that the sums of their variations are identical in each scenario. We assume that the hiring costs reductions are the same than in the benchmark model and thus are operative one month before the end of each lockdown. Figure 11 compares the TFP changes in the benchmark, a 3 month lockdown and a 6 months lockdown.

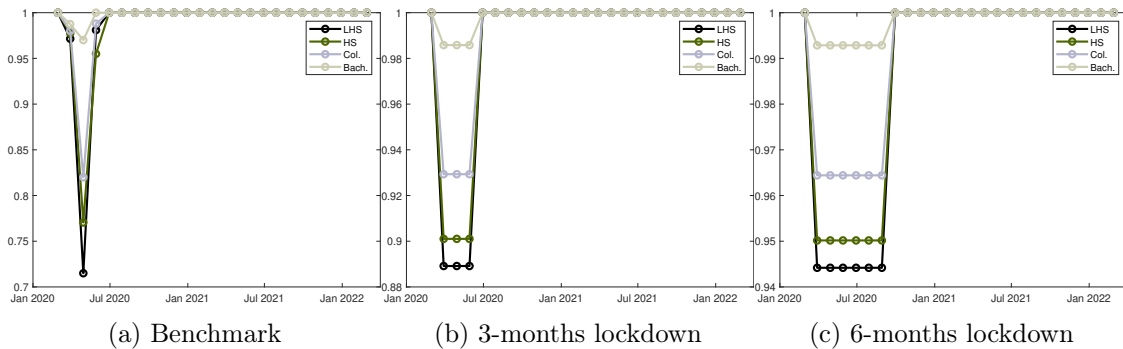


Figure 11: **TFP changes for different scenarios.**

Panels (a) and (d) of Figure 12 show that a longer but less strict lockdown (with the same TFP losses for all the scenarios) makes it possible to have a lower unemployment peak (+9.5pp or +6.5pp respectively for a lockdown of 3 or 6 months) than in the benchmark (+11.7pp). However, a 6-months lockdown implies a greater persistence of unemployment than shorter lockdowns (benchmark and 3 months). Thus, if extending the lockdown by making it less strict is beneficial at the start, this is no longer true beyond a certain length. These differences comes from the nonlinear impact of unemployment on hiring costs ( $\kappa_{s,t}$ ) and microeconomic risks ( $\sigma_{s,t}$ ).<sup>40</sup> The less stricter lockdowns, leading to lower unemployment increases, imply smaller changes in  $\kappa_{s,t}$  and  $\sigma_{s,t}$ . For a sufficiently large unemployment increase (the 3-months lockdown), the changes in microeconomic risk are dominated by the ones of unit hiring costs: with respect to the benchmark, the smaller raise in hiring costs allows the *JFR* to be larger<sup>41</sup>, explaining the smaller unemployment

<sup>39</sup>See Pissarides (2020), ch.2, for analytical derivations of these results.

<sup>40</sup>See Equations (1) and (3) for the links between unemployment rates and  $\kappa_{s,t}$  and  $\sigma_{s,t}$ .

<sup>41</sup>Smaller congestion externality than in the benchmark facilitates the hiring process. See section 4.2.

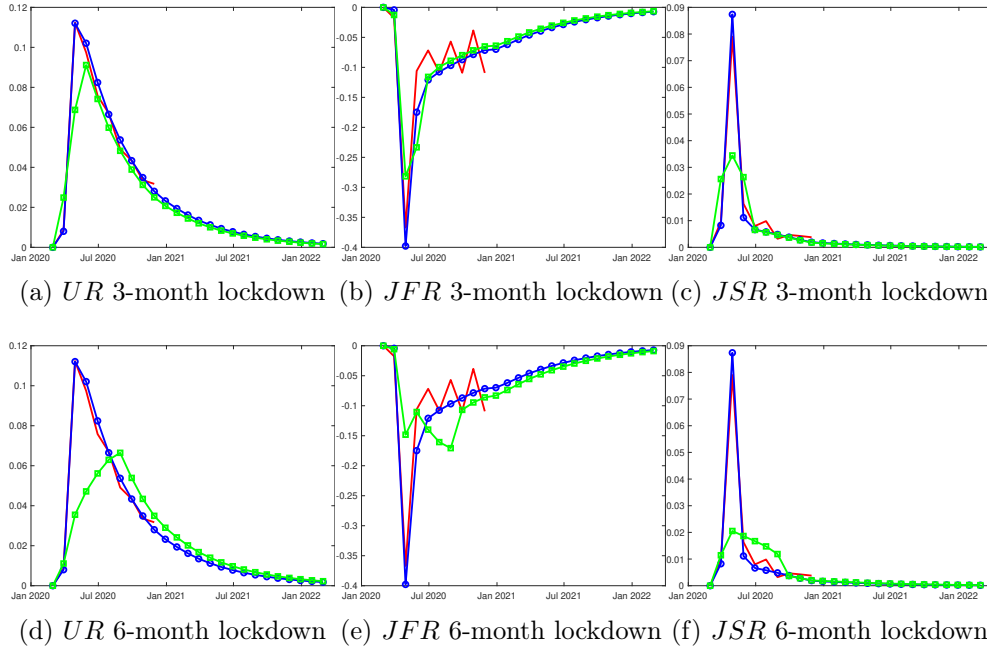


Figure 12: **Aggregate outcomes: longer but less stricter lockdown.**

persistence. At the opposite, when the raise in unemployment is sufficiently small (the 6-months lockdown), the changes in hiring costs are dominated by the ones of microeconomic risk: with respect to the benchmark, the smaller raise in microeconomic risk leads the *JFR* to be lower<sup>42</sup>, explaining the higher unemployment persistence.

Finally, using the same method than in section 4.1, Table 6 gives the wage losses in each scenario. Given that the lower unemployment persistence is in 3-month lockdown scenario, the lower wage losses are also reached in this scenario.

	LHS	HS	Coll.	Bach.	Total
Basic framework	-3.9%	-3.6%	-3.2%	-2.4%	-3.4%
3 months lockdown	-3.5%	-3.2%	-2.9%	-2.0%	-2.9%
6 months lockdown	-3.6%	-3.3%	-2.9%	-2.0%	-3.0%

Table 6: **Comparison of earning losses.** *Horizon of 24 months*

<sup>42</sup>The draws at the top of the distribution are reduced, and thus the expected profits. See section 4.2.

## 5 Conclusion

This study evaluates the impact of the COVID-19 crisis on the US labor market; it does so by using an extension of the Diamond–Mortensen–Pissarides model in a general equilibrium setup. We introduce several extensions: *(i)* heterogeneity of workers by education level, making it possible to combine heterogeneous adjustments in labor markets; *(ii)* endogenous separations, accounting for sharp increases in unemployment and business closures; *(iii)* time-varying microeconomic risks over the economic cycle; *(iv)* congestion externalities explaining the persistence of unemployment during recovery; and *(v)* wage rigidity, allowing the model to account for job separations even after the lockdown.

First, the model makes it possible to identify the size of the shocks needed to reproduce the first nine observed months of the crisis. Second, it predicts a highly persistent unemployment rate, despite the limited duration of the lockdown, with a return to the precrisis state in 2023. Finally, counterfactual simulations—in which one of the above extensions is shut down—stresses the importance of each one in explaining labor market dynamics.

Our work opens up the field to the question of how best to evaluate economic policies; future research that does so can benefit from the use of our structural model.



## References

- Adams-Prassl, A., Boneva, T., Golin, M. and Rauh, C. (2020), ‘Inequality in the Impact of the Coronavirus Shock: Evidence from Real Time Surveys’, *Journal of Public Economics* **189**.
- Adjemian, S., Karame, F. and Langot, F. (2019), On nonlinearities in the unemployment dynamic, mimeo, CEPREMAP.
- Attanasio, O. and Vissing-Jorgensen, A. (2003), ‘Stock-market participation, intertemporal substitution, and risk-aversion’, *American Economic Review* **93**(2), 383–391.
- Baker, R. S., Bloom, N., Davis, J. S. and Terry, J. S. (2020), COVID-Induced Economic Uncertainty, NBER Working Paper Series 27137.
- Barrero, J., Bloom, N. and Davis, J. (2020), COVID-19 Is Also A Reallocation Shock, NBER Working Paper Series 27137.
- Bartik, W., Bertrand, M., Lin, F., Rothstein, J. and Unrath, M. (2020), Measuring the labor market at the onset of the covid-19 crisis, NBER Working Paper Series 27613.
- Bernstein, J., Richter, A. and Throckmorton, A. (2020), COVID-19: A View from the Labor Market, Federal Reserve Bank of Dallas Working Paper 2010.
- Bick, A. and Blandin, A. (2020), Real-Time Labor Market Estimates During the 2020 Coronavirus Outbreak, Ssrn working paper.
- Birinci, S., Karahan, F., Mercan, Y. and See, K. (2020), Labor market policies during an epidemic, Federal Reserve Bank of New York Staff Reports 943.
- Blanchard, J. O. and Diamond, P. (1994), ‘Ranking, unemployment duration, and wages’, *The Review of Economic Studies* **61**, 417–434.
- Blanchard, O. and Gali, J. (2010), ‘Labor markets and monetary policy: A new keynesian model with unemployment’, *American Economic Journal: Macroeconomics* **2**, 1–30.
- Bloom, N. (2009), ‘The Impact of Uncertainty Shocks’, *Econometrica* **77**, 623–685.
- Bloom, N., Floetotto, M., Jaimovich, N., Saporta, E. and Terry, J. (2018), ‘Really Uncertain Business Cycles’, *Econometrica* **86**, 1031–1065.

- Cairo, I. and Cajner, T. (2016), ‘Human Capital and Unemployment Dynamics: Why More Educated Workers Enjoy Greater Employment Stability’, *The Economic Journal* **128**, 652–682.
- Chodorow-Reich, G. and Coglianese, J. (2020), Projecting Unemployment Durations: A Factor-Flows Simulation Approach With Application to the COVID-19 Recession, Working paper.
- Christiano, L., Eichenbaum, M. and Trabandt, M. (2016), ‘Unemployment and business cycles’, *Econometrica* **84**(4), 1523–1569.
- Cortes, G. and Forsythe, E. (2020), Impacts of the COVID-19 Pandemic and the CARES Act on Earnings and Inequality, IZA 13643.
- Daly, M., Hobbijn, B. and Lucking, B. (2012), Why has wage growth stayed strong?, Federal Reserve Bank of San Francisco Economic Letter. Issue Apr2.
- Den Haan, W., Ramey, G. and Watson, J. (2000), ‘Job destruction and propagation of shocks’, *American Economic Review* **90**, 482–498.
- Den Haan, W., Rendahl, P. and Freund, L. (2020), Volatile Hiring: Uncertainty In Search And Matching Models, CEPR 14630.
- Elsby, M. and Solon, G. (2019), ‘How prevalent is downward rigidity in nominal wages? international evidence from payroll records and pay slips’, *The Journal of Economic Perspectives* **33**(3), 185–201.
- Engbom, N. (2019), Application cycles, Society for Economic Dynamics 1170.
- Fana, M., Tolan, S., Torrejón, S., Brancati, U. and Fernández-Macías, E. (2020), The covid confinement measures and eu labour markets, JRC 120578.
- Ferraro, D. (2018), ‘The Asymmetric Cyclical Behavior of the U.S. Labor Market’, *Review of Economic Dynamics* **30**, 145–162.
- Ferraro, D. (2020), ‘Fast Rises, Slow Declines: Asymmetric Unemployment Dynamics with Matching Frictions’, *Journal of Money, Credit and Banking* **Forthcoming**.
- Gallant, J., Kroft, K., Lange, F. and Notowidigdo, M. (2020), Temporary Unemployment And Labor Market Dynamics During the COVID-19 Recession, NBER Working Paper series 27924.

- Gregory, V., Menzio, G. and Wicze, G. D. (2020), Pandemic recession: L or V-shaped?, NBER Working Paper Series 27105.
- Hall, R. (2017), ‘High discounts and high unemployment’, *American Economic Review* **107**, 305–330.
- Hall, R. E. (2005), ‘Employment fluctuations with equilibrium wage stickiness’, *American Economic Review* **95**(1), 50–65.
- Hall, R. E. and Milgrom, P. R. (2008), ‘The limited influence of unemployment on the wage bargain’, *American Economic Review* **98**(4), 1653–1674.
- Hall, R. and Kudlyak, M. (2020), Why Has the US Economy Recovered So Consistently from Every Recession in the Past 70 Years?, NBER Working Paper series 27234.
- Harding, J., Rosenthal, S. and Sirmans, C. (2007), ‘Depreciation of housing capital, maintenance, and house price inflation: Estimates from a repeat sales model’, *Journal of Urban Economics* **61**(2), 193–217.
- Jardim, E., Solon, G. and Vigdor, J. (2019), How Prevalent Is Downward Rigidity in Nominal Wages? Evidence from Payroll Records in Washington State, NBER Working Paper series 25393.
- Kapicka, M. and Rupert, P. (2020), Labor markets during pandemics, Mimeo. UC Santa Barbara.
- Krause, M. and Lubik, T. A. (2007), ‘The (ir)relevance of real wage rigidity in the new keynesian model with search frictions’, *Journal of Monetary Economics* **54**(3), 706–727.
- Kurmann, A. and McEntarfer, E. (2019), Downward Nominal Wage Rigidity in the United States: New Evidence from Worker-Firm Linked Data, Center for Economic Studies (Census) 19-07.
- Leduc, S. and Liu, Z. (2019), ‘The Weak Job Recovery in a Macro Model of Search and Recruiting Intensity’, **12**(1), 310–343.
- Lise, J. and Robin, J.-M. (2017), ‘The macro-dynamics of sorting between workers and firms’, *American Economic Review* **107**(4), 1104–1135.
- Martellini, P., Menzio, G. and Visschers, L. (2020), ‘Revisiting the Hypothesis of High Discounts and High Unemployment’, *The Economic Journal* .

- Molavi, P. (2018), A theory of dynamic selection in the labor market, Technical report, Department of Economics, MIT.
- Nicolas Petrosky, N. and Zhang, L. (2020), ‘Unemployment crises’, *Journal of Monetary Economics* **forthcoming**.
- Pissarides, C. (2020), *Equilibrium unemployment theory*, MIT Press.
- Robin, J.-M. (2011), ‘On the dynamics of unemployment and wage distributions’, *Econometrica* **79**(5), 1327–1355.
- Saez, E. and Zucman, G. (2014), Wealth inequality in the United States since 1913: Evidence from capitalized income tax data, NBER Working Paper Series 20625.

## A The first-order conditions of the firm's problem

Denoting  $\tilde{\alpha}_{s,t} = \frac{\int_{\alpha_{s,t}^r}^{+\infty} \alpha dG_{s,t}(\alpha)}{1 - G_{s,t}(\alpha_{s,t}^r)}$ , the production function is

$$Y_{s,t} = A_{s,t} A_t N_{s,t} \frac{1}{1 - G_{s,t}(\alpha_{s,t}^r)} \int_{\alpha_{s,t}^r}^{+\infty} \alpha dG_{s,t}(\alpha) = A_{s,t} A_t \tilde{\alpha}_{s,t} N_{s,t},$$

where  $A_{s,t}$  and  $A_t$  are the skill-specific and aggregate productivity, respectively. Denoting  $\tilde{w}_{s,t} = \frac{\int_{\alpha_{s,t}^r}^{+\infty} w_{s,t}(\alpha) dG_{s,t}(\alpha)}{1 - G_{s,t}(\alpha_{s,t}^r)}$ , the firm maximizes the following problem:

$$\begin{aligned} \mathcal{V}_{s,t}(N_{s,t}, A_t) &= \max_{V_{s,t}, N_{s,t}, \alpha_{s,t}^r} D_{s,t} + \tilde{\beta}_t \mathcal{V}_{s,t+1}(N_{s,t+1}, A_{t+1}) \\ \text{s.t.} &\begin{cases} D_{s,t} = N_{s,t} (p_{s,t} A_s A_t \tilde{\alpha}_{s,t} - \tilde{w}_{s,t}) - p_{s,t} \kappa_{s,t} V_{s,t} \\ N_{s,t+1} = (1 - s_{s,t+1})(N_{s,t} + q(\theta_{s,t}) V_{s,t}) \\ V_{s,t} \geq 0 \end{cases} \quad (\lambda_{s,t}) \end{aligned}$$

The first-order conditions (FOCs) are

$$0 = -p_{s,t} \kappa_{s,t} + q(\theta_{s,t}) \tilde{\beta}_t (1 - s_{s,t+1}) \frac{\partial \mathcal{V}_{s,t+1}}{\partial N_{s,t+1}} + \lambda_{s,t} q(\theta_{s,t}) \quad (7)$$

$$\begin{aligned} 0 &= \frac{\partial N_{s,t}}{\partial \alpha_{s,t}^r} (p_{s,t} A_s A_t \tilde{\alpha}_{s,t} - \tilde{w}_{s,t}) + N_{s,t} \left( p_{s,t} A_s A_t \frac{\partial \tilde{\alpha}_{s,t}}{\partial \alpha_{s,t}^r} - \frac{\partial \tilde{w}_{s,t}}{\partial \alpha_{s,t}^r} \right) \\ &\quad + \tilde{\beta}_t \frac{\partial \mathcal{V}_{s,t+1}}{\partial N_{s,t+1}} \frac{\partial N_{s,t+1}}{\partial N_{s,t}} \frac{\partial N_{s,t}}{\partial \alpha_{s,t}^r} \end{aligned} \quad (8)$$

$$\frac{\partial \mathcal{V}_{s,t}}{\partial N_{s,t}} = p_{s,t} A_s A_t \tilde{\alpha}_{s,t} - \tilde{w}_{s,t} + \tilde{\beta}_t (1 - s_{s,t+1}) \frac{\partial \mathcal{V}_{s,t+1}}{\partial N_{s,t+1}} \quad (9)$$

. The Kuhn–Tucker conditions are given by

$$q_s(\theta_{s,t}) V_{s,t} \geq 0, \quad \lambda_{s,t} \geq 0, \quad \text{and} \quad \lambda_{s,t} q_s(\theta_{s,t}) V_{s,t} = 0.$$

Knowing that  $1 - s_{s,t} = (1 - s_s)(1 - G_s(\alpha_{s,t}^r))$  and using

$$\begin{aligned} \frac{\partial N_{s,t}}{\partial \alpha_{s,t}^r} &= -(1 - s_s)(N_{s,t-1} + q(\theta_{s,t-1}) V_{s,t-1}) dG_s(\alpha_{s,t}^r) = -(1 - s_s) \frac{N_{s,t}}{1 - s_{s,t}} dG_s(\alpha_{s,t}^r) \\ \frac{\partial \tilde{\alpha}_{s,t}}{\partial \alpha_{s,t}^r} &= \frac{dG_s(\alpha_{s,t}^r)}{1 - G_s(\alpha_{s,t}^r)} (\tilde{\alpha}_{s,t} - \alpha_{s,t}^r) \\ \frac{\partial \tilde{w}_{s,t}}{\partial \alpha_{s,t}^r} &= \frac{dG_s(\alpha_{s,t}^r)}{1 - G_s(\alpha_{s,t}^r)} (\tilde{w}_{s,t} - w_{s,t}(\alpha_{s,t}^r)), \end{aligned}$$

the equation (8) can be rewritten as follows.

$$0 = p_{s,t} A_s A_t \alpha_{s,t}^r - w_{s,t}(\alpha_{s,t}^r) + \left( \frac{p_{s,t} \kappa_{s,t}}{q(\theta_{s,t})} - \lambda_{s,t} \right)$$

These FOCs of the firm's program lead to the following intertemporal job-destruction and job-creation conditions:

$$J_{s,t}(\alpha_{s,t}) = p_{s,t}A_{s,t}A_t\alpha_{s,t} - w(\alpha_{s,t}) + \tilde{\beta}_t(1 - s_{s,t+1})J_{s,t+1} \quad \forall \alpha_{s,t} \geq \alpha_{s,t}^r \quad (10)$$

$$J_{s,t}(\alpha_{s,t}^r) = 0 \quad (11)$$

$$J_{s,t} = p_{s,t}A_{s,t}A_t\tilde{\alpha}_{s,t} - \tilde{w}_{s,t} + \tilde{\beta}_t(1 - s_{s,t+1})J_{s,t+1} \quad (12)$$

$$\frac{p_{s,t}\kappa_{s,t}}{q(\theta_{s,t})} - \lambda_{s,t} = \tilde{\beta}_t(1 - s_{s,t+1})J_{s,t+1}, \quad (13)$$

where  $J_{s,t} = \frac{\partial \mathcal{V}_{s,t}}{\partial N_{s,t}}$  is the marginal value of employment, which can also be defined as  $J_{s,t} \equiv \frac{\int_{\alpha_{s,t}^r}^{+\infty} J_{s,t}(\alpha) dG_{s,t}(\alpha)}{1 - G_{s,t}(\alpha_{s,t}^r)}$ , where  $J_{s,t}(\alpha)$  is the marginal value of a job after the realization of the idiosyncratic productivity  $\alpha$ . Because  $J_{s,t}(\alpha) \geq 0$ ,  $\forall \alpha \geq \alpha_{s,t}^r$ , the average job value, defined by  $J_{s,t}$ , is necessarily positive. The intertemporal job-destruction condition indicates that the current losses ( $p_{s,t}A_{s,t}A_t\alpha_{s,t}^r - w_{s,t}(\alpha_{s,t}^r)$ ) must be compensated by the expected future gains generated by the job. The intertemporal job-creation condition equalizes the marginal costs of hiring at time  $t$  to the firm's marginal value of hiring, which is represented by the marginal benefits of hiring at time  $t+1$  discounted to  $t$  with the stochastic discount factor  $\beta$ . Hirings are based on the expectations of this average value of a job  $J_{s,t+1}$ , as  $\alpha$  is revealed after the contact.

Using the wage equation, and given that  $\alpha \in [0, +\infty)$  when the distribution is log-normal, the equilibrium reservation productivity is

$$\alpha_{s,t}^r = \max \left\{ 0; \frac{1}{(1 - \eta_s)p_{s,t}A_sA_t} \left[ (1 - \eta_s)b_s(A_t) + \eta p_{s,t}\kappa_{s,t}\theta_{s,t} - \left( \frac{p_{s,t}\kappa_{s,t}}{q(\theta_{s,t})} - \lambda_{s,t} \right) \right] \right\}.$$

The FOCs of the firm's program lead to the following intertemporal job-creation condition:

$$\frac{p_{s,t}\kappa_{s,t}}{q_s(\theta_{s,t})} - \lambda_{s,t} = \tilde{\beta}_t \left[ (1 - s_{s,t+1}) \left( p_{s,t+1}A_sA_{t+1}\tilde{\alpha}_{s,t+1} - \tilde{w}_{s,t+1} + \frac{p_{s,t+1}\kappa_{s,t+1}}{q_s(\theta_{s,t+1})} - \lambda_{s,t+1} \right) \right]$$

The Kuhn–Tucker conditions are given by

$$q_s(\theta_{s,t})V_{s,t} \geq 0, \quad \lambda_{s,t} \geq 0, \quad \text{and} \quad \lambda_{s,t}q_s(\theta_{s,t})V_{s,t} = 0.$$

When  $\lambda_{s,t} = 0$ , the equilibrium paths are the same as in the DMP model. When  $\lambda_{s,t} > 0$ , we have  $V_{s,t} = 0$ , and the solution is constrained with  $\theta_{s,t} = 0$  and  $N_t = (1 - s_s)(1 - G_s(\alpha_{s,t}^r))N_{s,t-1}$ .

## B Data

**Aggregate data.** The macro-level unemployment rate, job-finding rate, and job-separation rate data that we use are constructed from BLS data, from 1948 to the present. Data pertaining to monthly employment and unemployment levels for all people aged 16 and over are seasonally adjusted. To construct worker flows following Adjemian et al. (2019), we use the number of unemployed workers who have been unemployed for more than five weeks. After dividing the unemployment levels in each month by the sum of unemployment and employment, we obtain monthly series for  $U_m$  and  $U_m^5$  (where  $m$  refers to the monthly frequency); these correspond to the proportion of unemployed individuals and the proportion of individuals unemployed for more than five weeks, respectively. The worker flows are given by  $JSR_m = \frac{U_{m+1} - U_m^5}{E_m}$  and  $JFR_m = \frac{U_m - U_m^5}{U_m}$ .

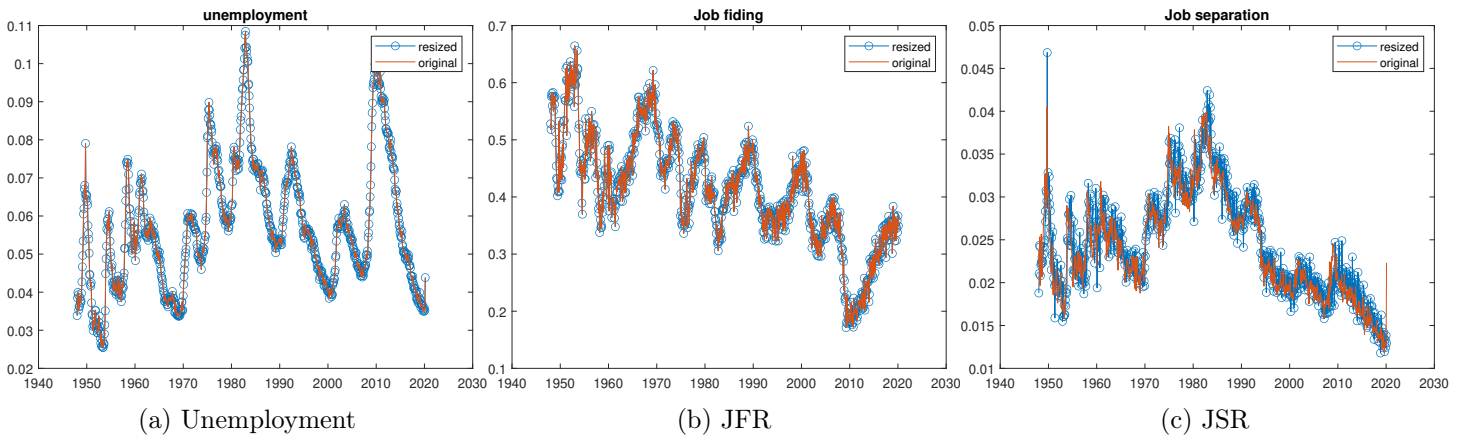
**Data by skill.** We use constructed data from Cairo and Cajner (2016), which are based on CPS basic monthly data from January 1976 to January 2014. They construct the number of short-term unemployed individuals (i.e., unemployed for fewer than five weeks) for each education group; doing so allowed them to calculate the heterogeneous job-finding and separation rates.

**Rescaling method.** To use both data sets, we first need to rescale them. We assume our aggregate data would remain unchanged.

First, we construct the artificial macro-level unemployment rate ( $bur_t$ ,  $bjsr_t$ , and  $bjfr_t$ ) by using micro data ( $ur_{s,t}$ ,  $jsr_{s,t}$ , and  $jfr_{s,t}$ ) and the weight of each skill in the economy  $\omega_s$ :  $bur_t = \sum_{s=1}^S \omega_s ur_{s,t}$ ,  $bjsr_t = \sum_{s=1}^S \omega_s jsr_{s,t}$ , and  $bjfr_t = \sum_{s=1}^S \omega_s jfr_{s,t}$ . We then calculate the coefficient of rescaling  $x^i$  such that  $x_{s,t}^1 = jfr_{s,t}/bjfr_t$ ,  $x_{s,t}^2 = ur_{s,t}/bur_t$ , and  $x_{s,t}^3 = jsr_{s,t}/bjsr_t$ .

Second, we reconstruct the micro data to match the macro data ( $UR$ ,  $JFR$ , and  $JSR$ ):  $hjsr_{s,t} = x_{s,t}^1 JFR_t$ ,  $hur_{s,t} = x_{s,t}^2 UR_t$ , and  $hjsr_{s,t} = x_{s,t}^3 JSR_t$ .

Finally, to test our estimation, we calculate the macro data using the rescaled micro data:  $hbur_t = \sum_{s=1}^S \omega_s hur_{s,t}$ ,  $hbjfr_t = \sum_{s=1}^S \omega_s hjsr_{s,t}$ , and  $hbjsr_t = \sum_{s=1}^S \omega_s hjsr_{s,t}$ ; we then compare these data to the original data ( $UR$ ,  $JFR$ , and  $JSR$ ). We find that the rescaling matches the data well.



(a) Unemployment

(b) JFR

(c) JSR



## C Steady-state restrictions identifying $\eta_s$ and $b_s$

We use the two FOCs of the firm's program with respect to  $\theta_{s,t}$  and  $\alpha_{s,t}^r$  to identify two parameters in each sector. We choose to identify  $\eta_s$  and  $\tilde{b}_s \equiv b_s/(p_s A_s)$ , which are thus skill-specific. If we assume that the steady-state value of  $\kappa_s$  is proportional to  $A_s$ , s.t.  $\kappa_s = k A_s$ , then we identify  $\eta_s$  as follows.

$$\eta_s = 1 - \frac{k}{q_s(\theta_s)\beta(1 - jsr_s)(\tilde{\alpha}_s - \alpha_s^r)},$$

where  $k$  is chosen s.t.  $\frac{\sum_s \omega_s N_s \eta_s}{\sum_s \omega_s N_s} = 0.5$ , leading to  $k = 0.103$ . The other FOC allows us to identify  $\tilde{b}_s = \frac{b_s}{p_s A_s}$ :

$$\tilde{b}_s = \alpha_s^r - \frac{\eta_s}{1 - \eta_s} k \theta_s + \frac{1}{1 - \eta_s} \frac{k}{q(\theta_s)},$$

which leads to a ratio of home production to production in business of  $\tilde{b}_s/\tilde{\alpha}_s$ .

## D The fit of the 2008 crisis

Figure 13 presents the results and shows that the model can match the dynamics of the four labor markets (LHS, HS, Coll., and Bach. or more).

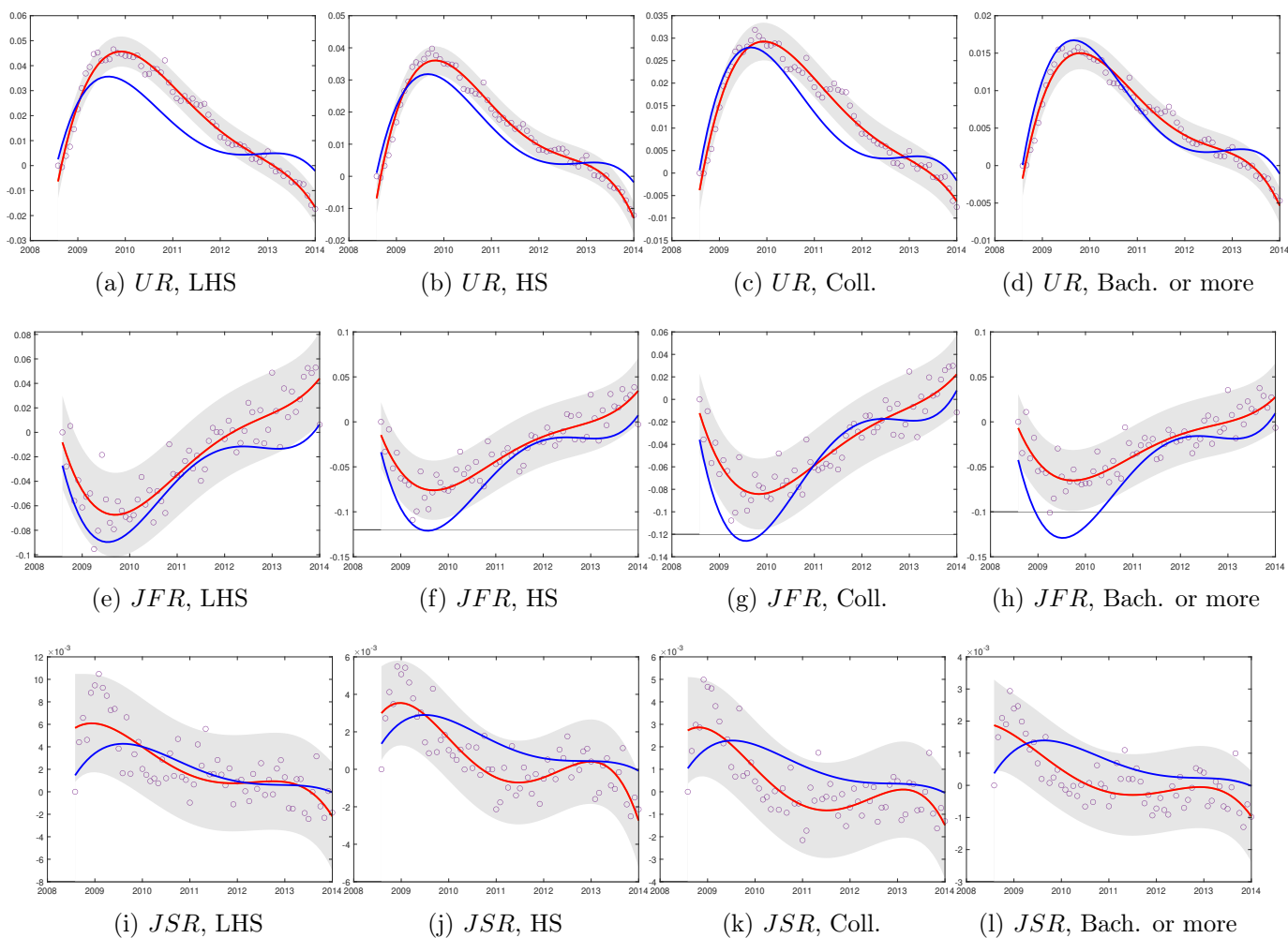


Figure 13: **Worker flows and stock by education level.** The circles represent the raw monthly data leading to smoothed polynomials (in red), with confidence bands (95%) (in gray). The blue lines represent smoothed polynomials generated by the model.

Figure 14 illustrates the accuracy of our model results, as it compares our predictions to aggregate indicators of the US labor market.

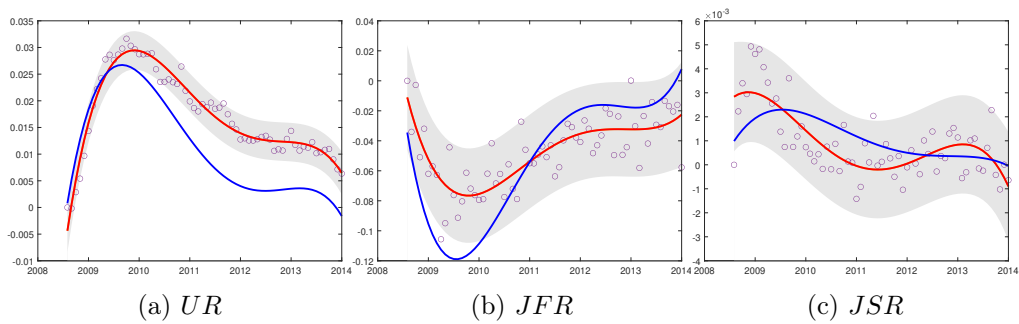


Figure 14: **Aggregate worker flows and stock.** In Panels (a)–(c), the circles represent the raw monthly data leading to smoothed polynomials (in red), with confidence bands (95%) (in gray). The blue lines represent the smoothed polynomials generated by the model.

## E Labor market indicators of the benchmark model

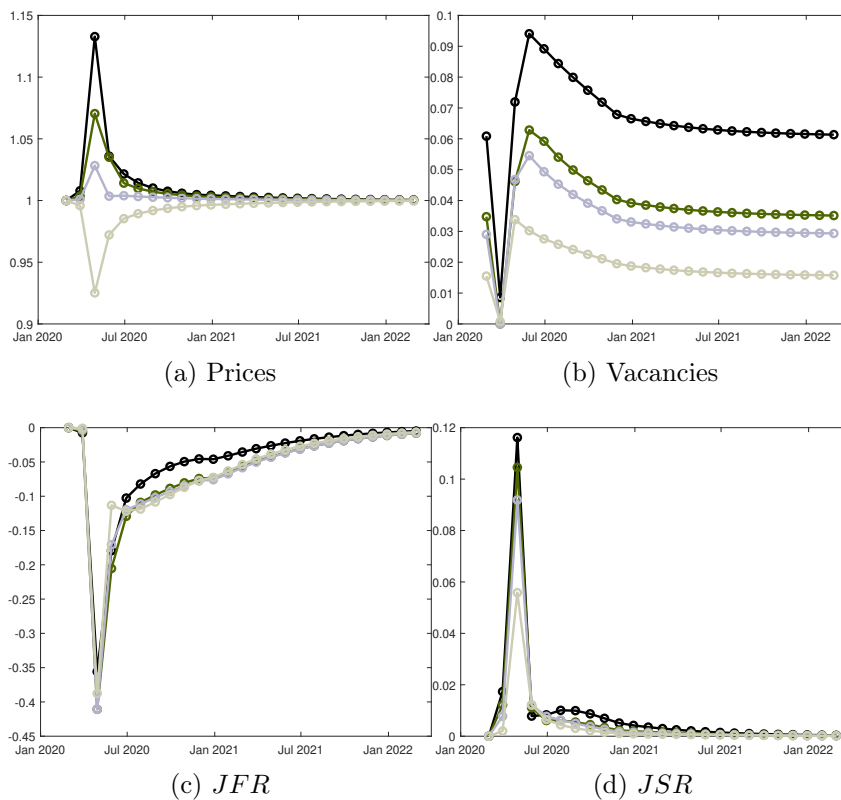


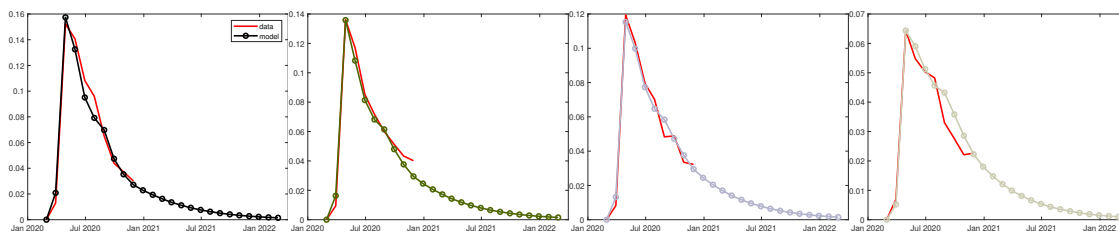
Figure 15: **Outcomes by education level.** Panels (a)–(d): Black lines for the less than high school diploma (LHS); Khaki lines for the for the high school diploma (HS); Gray lines for the college diploma (Coll.); Camel lines for the bachelor degree or more (Bach.).

## F Model calibration when one extension is removed

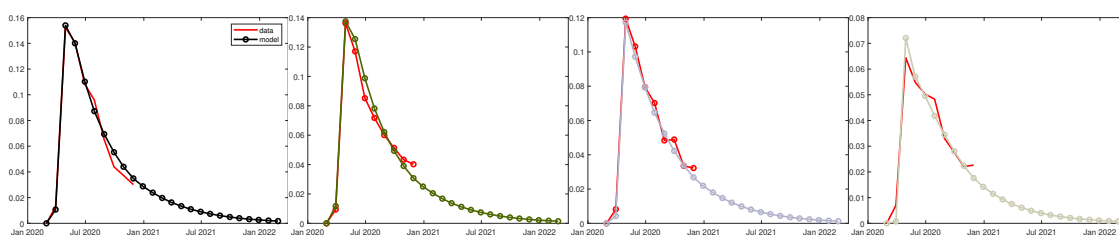
	Mar	Apr	May	Jun	Jul	Aug	Sep	Oct
	<b>Less than High School</b>							
Basic Framework	-0.0285	-0.285	-0.019	0	0	0	0	0
No congestion on hiring costs	-0.0285	-0.133	-0.095	-0.038	-0.038	-0.038	0	0
No wage rigidity	-0.0285	-0.380	0	0	0	0	0	0
No uncertainty	-0.0285	-0.323	0	0	0	0	0	0
	<b>High School</b>							
Basic Framework	-0.0225	-0.2295	-0.045	0	0	0	0	0
No congestion on hiring costs	-0.0225	-0.0990	-0.027	-0.009	-0.009	-0.009	0	0
No wage rigidity	-0.0225	-0.3600	0	0	0	0	0	0
No uncertainty	-0.0225	-0.3150	0	0	0	0	0	0
	<b>College</b>							
Basic Framework	-0.02	-0.1800	-0.0120	0	0	0	0	0
No congestion on hiring costs	-0.02	-0.0480	-0.0160	0	0	0	0	0
No wage rigidity	-0.02	-0.1880	0	0	0	0	0	0
No uncertainty	-0.02	-0.2608	0	0	0	0	0	0
	<b>Bachelor and more</b>							
Basic Framework	-0.0125	-0.0300	0	0	0	0	0	0
No congestion on hiring costs	0	0.0250	0.0375	0.015	0.01	0	0	0
No wage rigidity	0	0	0	0	0	0	0	0
No uncertainty	-0.0125	-0.0375	-0.0250	-0.020	-0.015	-0.01	-0.01	-0.01

Table 7: **Productivity loss**

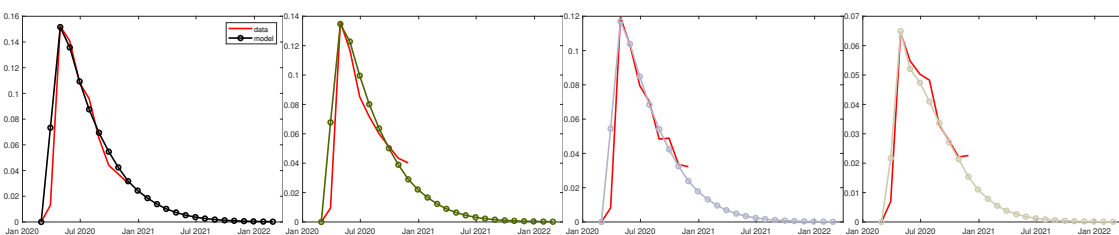
## G Model fit when one extension is removed



(a) Hiring cost: *LHS* (b) Hiring cost: *HS* (c) Hiring cost: *Coll.* (d) Hiring cost: *Bach*



(e) Wage rigidity: *LHS* (f) Wage rigidity: *HS* (g) Wage rigidity: *Coll.* (h) Wage rigidity: *Bach*



(i) Varying risk: *LHS* (j) Varying risk: *HS* (k) Varying risk: *Coll.* (l) Varying risk: *Bach*

Figure 16: **Unemployment rate by education level.** In Panels (a)–(l), the red lines represent the data.

## H Counterfactual simulation

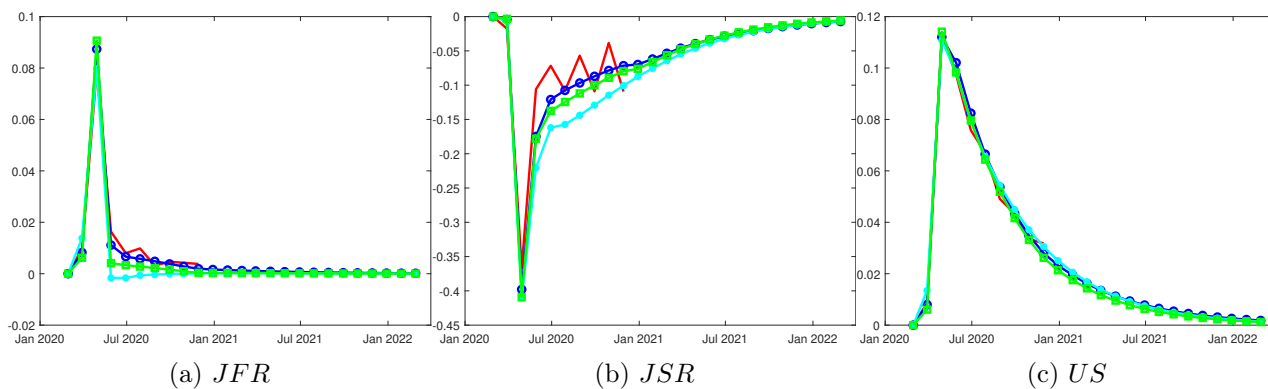


Figure 17: **Simulation without wage rigidity and hiring costs subsidies.** In Panels (a)–(c), the red lines represent the data, the blue lines represent the benchmark model, the green lines represent the model without wage rigidity and the turquoise lines represent the model without wage rigidity and hiring costs subsidies.